D3.2 REPORT ON TERMINALS

Revision: 1.0

Work package	WP 3
Task	Task 3.2
Due date	30/06/2024
Submission date	05/08/2024
Deliverable lead	Greenerwave
Version	1.0
Authors	Greenerwave, Telit (Florian Denzin, Volker Breuer), Ericsson (Eduardo Medeiros, Per-Erik Eriksson, Sebastian Euler), Ericsson France (Ioannis Xirouchakis), CTTC, Thales, DLR
Reviewers	Joel Grotz (SES), Laurent Reynaud (Orange), Madivanane Nadarassin (Thales)
Abstract	The following deliverable focuses on the main evolution and innovation area for 6G-NTN terminals. Innovative antenna design was identified to bear most technological potential for improved terminal characteristics for 6G NTN system.
Keywords	6G-NTN, terminals, antenna, antenna design

Grant Agreement No.: 101096479
Call: HORIZON-JU-SNS-2022

Topic: HORIZON-JU-SNS-2022-STREAM-B-01-03
Type of action: HORIZON-JU-RIA

Document Revision History

Version	Date	Description of change	List of contributor(s)
V0	25/01/2024	Initial Report Structure	Volker Breuer, Florian Denzin (Telit)
V0.10	01/08/2024	Review and formatting	Valentina Margaria…
V1.0	05/08/24	Approval and submission	Alessandro Vanelli-Coralli (UniBo)

DISCLAIMER

Co-funded by the European Union

6GSNS

Project funded by

Schweizerische Eidgenossenschaft
Confédération suisse
Confederazione Svizzera
Confederaziun svizra

Swiss Confederation

Federal Department of Economic Affairs, Education and Research EAER
State Secretariat for Education, Research and Innovation SERI

6G-NTN (*6G Non Terrestrial Network*) project has received funding from the **Smart Networks and Services Joint Undertaking (SNS JU)** under the European Union's **Horizon Europe research and innovation programme** under Grant Agreement No 101096479. Views and opinions expressed are however those of the author(s) only and do not necessarily reflect those of the European Union. Neither the European Union nor the granting authority can be held responsible for them. This work has received funding from the Swiss State Secretariat for Education, Research and Innovation (SERI).

COPYRIGHT NOTICE

Project co-funded by the European Commission in the Horizon Europe Programme		
Nature of the deliverable:	**R**	
Dissemination Level		
PU	*Public, fully open, e.g., web (Deliverables flagged as public will be automatically published in CORDIS project's page)*	✓
SEN	*Sensitive, limited under the conditions of the Grant Agreement*	
Classified R-UE/ EU-R	*EU RESTRICTED under the Commission Decision No2015/ 444*	
Classified C-UE/ EU-C	*EU CONFIDENTIAL under the Commission Decision No2015/ 444*	
Classified S-UE/ EU-S	*EU SECRET under the Commission Decision No2015/ 444*	

* R: Document, report (excluding the periodic and final reports)

DEM: Demonstrator, pilot, prototype, plan designs

DEC: Websites, patents filing, press & media actions, videos, etc.

DATA: Data sets, microdata, etc.

DMP: Data management plan

ETHICS: Deliverables related to ethics issues.

SECURITY: Deliverables related to security issues

OTHER: Software, technical diagram, algorithms, models, etc.

EXECUTIVE SUMMARY

This is an intermediate report related to terminal consideration and investigations related to 6G-NTN. In the initial evaluation, the user requirements and the related KPIs identified in context of deliverable D2.1, D2.2 and D2.3 are mapped against potential different terminal types.
For the lower frequency ranges (sub 6GHz), narrowband communication being integrated into terminals seems to be a logical decision for price/bill of material, wide user acceptance and distribution reasons for 6G-NTN capable terminals.
For wideband communication, terminals in a higher frequency range (>10GHz) are considered. When evaluating the related requirements in terms of throughput and other requirements, it becomes obvious that today's terminal designs done for 5G terrestrial networks in FR2 suit to a large extend the required needs especially concerning throughput processing capability and performance. A certain frequency adaptation to operate in C or Q/V band needs to be done but overall todays existing terminals include most of the parts required to fulfill such performance needs.
This similarity and the ability of re-use of existing terminal concepts is also a key factor to success, when re-using hardware components known from other commercial terminal designs (e.g., 5G terrestrial).
The main difference and component bringing most innovation and improvement potential compared to existing terminal concepts, was identified to be the antenna design. New and innovative antenna design can bring the required gain to increase the throughput performance while respecting the geometry dimensions assessed and evaluated for several of the analyzed use cases (e.g., automotive, drones).
Consequentially antenna simulations and design, considering the user and use case requirements (geometry) and their corresponding realization including corresponding measurements will be the main focus to achieve the ambitious performance/throughput increase intended for 6G-NTN wideband communication.

TABLE OF CONTENTS

LIST OF FIGURES

LIST OF TABLES

ABBREVIATIONS

3D	3-Dimensional
6G	Sixth Generation
3GPP	3rd Generation Partnership Project
AI	Artificial Intelligence
ACLR	Adjacent Channel Leakage power Ratio
ACU	Antenna Control Unit
AFS	Antenna Feeder System, Antenna Feeding System
AI	Artificial Intelligence
ASIC	Application-Specific Integrated Circuit
BOM	Bill Of Material
BS	Base station
BVLoS	Beyond Visual Line of Sight
BW	Bandwidth
BWP	Bandwidth Part
C2	Command and Control
C2CSP	C2 Link communication service provider
CA	Carrier Aggregation
CC	Component Carrier
CMOS	Complementary Metal-Oxide-Semiconductor
COTS	Commercial off-the-shelf
CoW	Cell on Wheels
C-SWaP	Cost Size Weight and Power
CW	Continuous Wave
C2	Command and Control
C2CSP	C2 Link communication service provider
DC	Direct Current
DL	Downlink

DMA	Dynamic Metasurface
DS	Discrete Source
EAB	External Advisory Board
E-tan	Tangential Electric Field
EASA	European Union Aviation Safety Agency
EIRP	Equivalent Isotropic Radiated Power
EIS	Effective Isotropic Sensitivity
E2E	End-to-end
FDD	Frequency-Division Duplexing
FM/AM	Frequency Modulation/Amplitude Modulation
FPA	Fabry Perot Antenna
FR	First Responder
FR2	Frequency Range 2 according 3GPP
GEO	Geostationary Earth Orbit
gNB	Next-generation Node-B
GND	Ground
GNSS	Global Navigation Satellite Systems
GPS	Global Positionning System
GSO	Geostationary Orbit
HAP	High Altitude Platform
H-Pol	Horizontal Polarization
HV	Host Vehicle
HW	Hardware
IC	Integrated Circuit
IF	Intermediate Frequency
IoT	Internet of Things
ISL	Inter-Satellite Link
KPI	Key Performance Indicator
LC	Liquid Crystal

LEO	Low Earth Orbit
LO	Local Oscillator
LoS	Line of Sight
MBW	Measurement Bandwidth
MEMS	Micro-Electro-Mechanical Systems
MEO	Medium Earth Orbit
MFCN	Mobile/Fixed Communications Networks
mMTS	Mini-Metasurface
MNO	Mobile Network Operator
MTS	Metasurface
NF	Near-Field
NGSO	Non-Geostationary Orbit
NLoS	Non-Line of Sight
NR	New Radio
NTN	Non-Terrestrial Network
OBW	Occupied Bandwidth
OCNG	OFDMA Channel Noise Generator
OFDMA	Orthogonal Frequency-Division Multiple-Access
OTA	Over-The-Air
OoB	Out-of-Band
OoBE	Out-of-Band Emission
PAPR	Peak-to-Average Power Ratio
PCB	Printed Circuit Board
PIN diode	Positive-Intrinsic-Negative diode
PPDR	Public Protection and Disaster Relief
PPM	Parts per million
PRB	Physical Resource Block
PSD	Power Spectrum Density
PTT	Push-To-Talk

QoE	Quality of Experience
QoS	Quality of Service
RB	Resource Block
Rel	Release
RF	Radio Frequency
RIB	Radiated Interface Boundary
RIC	Radio Intelligent Controller
RIS	Reconfigurable Intelligent Surface
RL	Return Loss
RPE	Radiated Power Envelope
Rx	Receiver
SAN	Satellite Access Node
SAR	Search and Rescue
SCS	Subcarrier Spacing
SE	Spurious Emission
SI	Study Item
SON	Self-organizing networks
SOTM	Satellite-On-The-Move
TE	Transverse Electric field
TM	Transverse Magnetic Field
TN	Terrestrial Network
TR	Technical Report
TRP	Total Radiated Power
Tx	Transmit, transmitter
TS	Technical Specifications
UAM	Urban Air Mobility
UAV	Uncrewed Aerial Vehicle
UAV-C	UAV Controller
UC	Use Case

UE	User Equipment
UL	Uplink
UOF	Uniformity of the field
USAT	Ultra-Small-Aperture Terminal
VICTS	Variable Inclination Continuous Transverse Stub
vLEO	Very Low Earth Orbit
VLoS	Visual Line of Sight
VNA	Vector Network Analyzer
VNF	Virtualized Network Function
V-Pol	Vertical Polarization
X-Pol	Cross Polarization
VR	Virtual Reality
VSAT	Very-Small-Aperture Terminal
VTOL	Vertical Take-Off and Landing
WI	Work Item
WP	Work Package

1 INTRODUCTION

In relation to the work performed in WP2, and its deliverables: use cases (D2.1), user requirements (D2.2) as well as system requirements (D2.3) related to terminal expectations, the requirements and identified terminal types for user perspective will be translated to technical terminal types and their characteristics will be further analyzed and evolved.

The requirements on user equipment results in various technical terminal options. The terminal options found to be most relevant will be further assessed especially with regard to new technical challenges and innovation potential.

In addition, implementation constraints related to common TN and NTN usage terminals and separate standalone NTN usage especially for broadband use cases have to be considered. Similarity to existing TN terminals, such considerations are important for mass production and success of NTN. Therefore, adaptation and implementation to cell phones is one aspect.

Even for challenging wideband NTN throughput realization in higher frequency ranges (Q and V band), a similarity of most terminal components regarding amplifiers is deemed beneficial. The usage of state of the art-components for most of the terminal parts in the various terminal designs is important to allow for potential mass production. Consequentially, the antenna design is identified as the terminal component bearing the most innovative potential for leading to higher throughput and coverage values for 6G-NTN.

Antennas are identified as main improvement area and hence will be main contribution section to 6G NTN performance and consequentially being in major focus for terminals.

The state of the art and existing requirements are recapitulated keeping in mind the use case and requirement-driven constraints, evaluated and captured in the deliverables D2.1, D2.2 and D2.3, especially with respect to dimensioning are considered.

The major task is to identify new antenna design concepts having advantageous characteristics for broadband NTN usage. As previously mentioned, such designs are susceptible to convey major improvement potential.

It needs to be noted that this is an intermediate report and not all wideband antenna options (C band, Q/V band) will be captured in this report. In this first phase, the emphasis was on technological developments, and further investigations will be made based on these intermediate results. Necessary conclusions on efficiency, sustainability and recyclability will be captured in the final report and only briefly assessed here within. Finally, only first feedback from EAB (External Advisory Board) on the conducted antenna analysis and dimensioning activity will be captured.

1.1 SCOPE AND OBJECTIVES

In general, the NTN frequency range can be divided into the lower frequency range i.e. sub 6GHz consisting of S, L and also C band (which is in current consideration for NTN), and a higher frequency range above 6GHz consisting of the Q/V band compare table 1. The 6G NTN frequency band study work is treated in detail in context of deliverable D2.5 “Policies and Regulatory analysis”.

Each of these frequency ranges has its own constraints with respect to the terminal design and is adopted in different use cases. The sub-6GHz range for NTN is mainly intended for handhelds, being often dual design with terrestrial usage. Hence the used components and antenna design are mainly the same as those used for the TN usage, as NTN in these devices only gets widely adapted if no further hardware (HW) constraints impacting terminal cost are

placed. However, in these scenarios as well, 6G-NTN achieves new throughput experiences. However, they are not centered at the terminal side but rather from the 6G-NTN system design. Hence, they will be evaluated in general in context of the 6G-NTN project but are not in the scope of the terminal studies.

For the Q/V and C band most likely assumptions of technical realization with respect to amplifier in receiving and transmitting path are considered being based on state-of-the-art, as amplifiers have a slow innovation slope being already followed since years within other studies and projects.

The major investigation scope to fulfill the user requirements and achieve increased throughput compared to state-of-the-art NTN systems is within new antenna designs for Q/V and C band fulfilling the user requirements concerning size and throughput needs.

The achieved antenna performance will be compared to existing state-of-the-art antenna performance requirements and will serve as further basis for link-level and system-level assessment of 6G NTN within the further project.

In this first report, especially the study results on antenna investigations for the Q/V band are presented starting with the larger dimensioning size for the user requirements.

1.2 STRUCTURE OF THE DOCUMENT

This deliverable is structured as follows:

- **Section 1**
- Introduction and scope.
- **Section 2**
- A closer examination of UE types, their characteristics and potential implementation and band usage in devices. Translation of the findings into an investigation scope and consideration of existing 3GPP requirements for comparison.
- A look at the relevant bands for the 6G NTN project and the bandwidth and RF characteristics and requirements.
- **Section 3**
- A survey on antenna technology for the C and Q/V band outlining the state of the art. A focus are the different types of beam forming implementations and how they are realized. Followed by a critical analysis for the Q/V and C band solutions and resulting challenges.
- **Section 4**

Description and results of the antenna investigation with the objectives based on the considerations of Part 2 and Part 3 of the D2.3 document. The investigation explores the usage of Metasurface for the antenna design. Simulations as well measurements of the antenna samples are documented.

2 SELECTED UE TYPES, CAPABILITIES AND SWAP CHARACTERISTICS

2.1 INTRODUCTION

Mobile communication terminals exist for various technologies and purposes, however a terminal for mobile communication typically consists of some commonly used building blocks. A terminal typically consists of a modem, a receiver and transmitter circuitry and corresponding antennas. For a better understanding a schematic is depicted below.

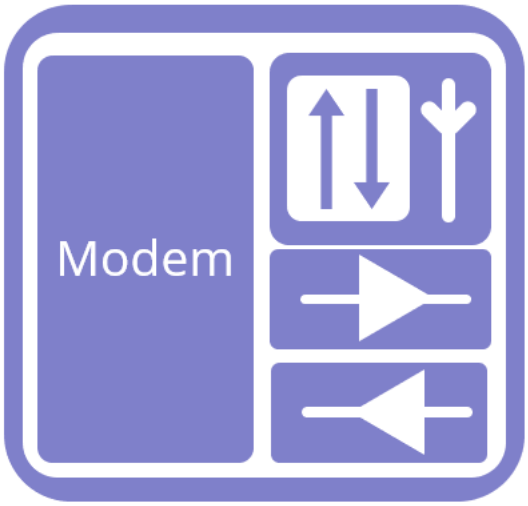

Figure 1: SCHEMATIC DRAWING OF A TERMINAL

The modem has the task to process the received data and even though modulation and coding for 6G-NTN may not be clear be now, based on expected throughput for 6G-NTN today's modem processing capabilities for 5G terrestrial networks also including frequency range 2 (FR2) are able to cope with such high throughputs and even much higher data capabilities.

The receiving and transmit circuitry mainly consists of receive and transmit amplifier providing corresponding amplification and noise figure (receiver) being suitable for mobile communication. Transmitter and receivers of various sizes exist today, also in the considered frequency ranges. Hence the state-of-the-art of such receivers and transmitters can be referred to., The selection for the respective terminal types used within a certain use case, also depends on additional aspects such as deployment, usage conditions or power consumption. Amplifier development is a separate general evolution topic and hence in context of 6G-NTN terminal considerations, reference will be made to available state-of-the art for the respective terminal types and use case scenario.

Receive and transmit antennas are a crucial topic with respect to use case KPIs and user acceptance giving that their performance directly impacts achievable data throughput, and its dimension and weight directly impacts use case scenario and user experience.

Furthermore, the requirements for the antenna heavily depend on the use case, intended throughput, level of integration and further use case dependent aspects, hence playing a major role and for new or enhanced 6G NTN use cases being a key element for innovation.

In this section the outcome of WP 2.1 and WP 2.2. will be analyzed and translated/classified into technical terminal requirements. It will be shown that several of the UE types identified in WP 2.1 and WP2.2 will translate into the same technical terminal type and just will fulfill different use needs by different packaging. Especially a grouping of the terminals with respect to the usage as broadband or integrated narrowband communication terminal and their characteristics with respect to terminal antenna requirements will be made. Furthermore, the state-of-the-art terminal/UE requirements of 3GPP for existing NTN systems will be referenced to guide towards the innovative field of antenna analysis and show the increase in throughput and coverage that can be achieved with a 6G NTN system making use of such new antenna designs.

2.2 OVERVIEW ON UE TYPES AND THEIR REQUIREMENTS

In context of D2.2 following UE types were distinguished handheld, drone and mounted devices. Each of the types is differentiated into two subclasses: commercial and professional handheld, respectively small or large drones and first responder stationery or mounted devices. The corresponding segmentation is depicted in the figure below

Figure 2: UE types according to D2.2

When analyzing the characteristics, it can be seen that only two basic terminal types need to be distinguished where one of these types can further be distinguished by a slight differentiation concerning acceptance for size and weight.

The commercial handheld refers to a design which has dual-use capabilities for TN and NTN networks intended for the sub-6GHz range i.e., being based on a classical integrated front end on handhelds. In that context, the used components (receive and transmit amplifiers as well as the antenna design) are bound to the typical values which are achievable for today's commercial handhelds i.e. 23dBm amplification, 9dB receiver noise figure and -3dBi antenna gain. Such a terminal design making use of commercial handheld constraints allows for NTN

narrowband communication by making use of the satellite bands in the sub-6GHz range (S and L band). As being bound in its components to commercial used terrestrial handheld designs and being limited in antenna design due to dimension limitation of the UE type a performance increase for this device type in 6G NTN will mainly come from other system elements besides the terminal. Even though being an important type for 6G NTN, this UE type is of lower interest in the further terminal study due to its design limitations and the economy of scale pressure for this type of handheld devices.

Also, the professional handheld can be considered as being part of that category, being a slightly larger dimensioned handheld terminal allowing for slightly more weight than consumer handhelds and providing slightly increased RF performance with power amplifiers (26dBm) acceptable for use in proximity of a human head for limited time and intensity.

Mounted devices (e.g., cars, trains) or stationary first responder devices refer in principle to the same terminal type being larger in dimension especially for the antenna design and heavier in weight. In this regard, it is worth highlighting that mounting antennas of mounted devices or stationary installations on a roof top can ensure better visibility to the satellite C band for vehicular, light drone, train and maritime backup can be considered with slightly improved antennas on 0dBi and larger power amplifiers (typically 26dBm), where the additional antenna gain is mainly due to improved efficiency.

Wideband and ultra-wideband communication mounted devices (e.g., trains, large drones and vessels) is a second terminal where achieving a high throughput is one of the major KPIs. This type of device can be heavier in weight and larger in dimension (which, in the context of Q/V band usage for wideband and ultra-wideband communication, can allow larger RF amplifier and antenna to overcome the higher attenuation). The mounted devices can be distinguished in a intermediate variant allowing for 20X20cm design and a smaller variant allowing for 10x10cm design. The dimension also refers to the acceptable antenna size being far larger than modem and respective device design (including amplifiers). These devices also need to support wideband communication, which includes at least C or even Q/V band i.e., realization of the support of higher frequency ranges and having superior antenna characteristics being directly related to the achievable throughput.

For wideband support in the Q/V band, even though larger power amplifiers can be used (up to 34 or even 37dBm) for certain use cases such as trains and vessels or large drones, i.e. allowing for mounting not in proximity of the human head because of healthcare considerations. The corresponding sustainability requirements are expressed in D2.3 page 55 (§4.4) : STR-SUST-07 ("The 6G-NTN system shall be able to assess and minimize its impact regarding EMF exposure") and STR-SUST-08 ("The 6G-NTN system shall follow the existing international and national 6G EMF-awareness guidelines (e.g., those of ICNIRP [12] [13]). It is obvious that a larger benefit for link level/throughput considerations, especially for these bands is related to the usage of corresponding high performing antennas.

See also D2.3 page 55 (§4.4) : STR-SUST-07 ("The 6G-NTN system shall be able to assess and minimize its impact regarding EMF exposure") and STR-SUST-08 ("The 6G-NTN system shall follow the existing international and national 6G EMF-awareness guidelines (e.g., those of ICNIRP [12] [13])."

A mapping of the UE types assessed in 2.2. to the terminal types described with their main characteristics is presented in the table hereafter. See also to D2.3 section 3.4.1 Considered UEs, with Table 1 "TARGET UE DESIGNS DEFINED IN T3.2 (COLUMN 2), WITH A MAPPING OF THE USAGE-BASED UE CATEGORIES FROM D2.2"

Table 1: Mapping of UE types to terminal types and their characteristics

UE type	Communication characteristics	Terminal type	RF characteristic	Frequency band
Handheld	narrowband	classical integrated front end on handheld	typ. NF=9 Gain : -3dBi, Tx=23 dBm	Sub 6GHz S and L band
Professional handheld	Narrowband medium	Enhanced RF front end	typ. NF=7 Gain : -3dBi, Tx=26 dBm	Sub 6GHz C band
Drone; car (small mounted UE)	medium	Enhanced Rf and antenna	typ. NF=7 Gain : 0 dBi, Tx =26 dBm	Sub 6GHz C band
Drone, train vessel (mounted UE)	wideband	Enhanced RF and improved noise figure performance	typ. NF=5; Tx =25,5 dBm	Q/V band
Drone, train vessel (mounted UE)	Ultra-wideband	Enhanced RF and extreme noise figure performance	typ. NF=4; Tx =28 dBm	Q/V band

Handheld fully integrated, has not been within the scope of D3.2 Terminals.

For professional handled and car C band is not yet studied in the antenna section and may be referred to in the final report for antenna evaluation.

Drone, train and drone, vessel to be studied in this report.

As can be seen from the table above, for commercial handhelds, their tight restrictions set on the used components being used for classical integrated frontends. But also, for other terminal types with respect to receive or transmit amplifiers/circuitry to state-of-the-art levels achievable with commercially available devices is made. Only be relying for those devices also majorly impacting the terminal BOM (Bill Of Material) it will be feasible to enhance existing handhelds by integrations and serving further standalone or combined use cases with terminals available at a reasonable price point.

For wideband and ultra-wideband communication not being bound to common TN/NTN handheld or general designs constraints, an improved antenna characteristic within the dimensions given for the use cases (D2.2) and UE types to be acceptable, i.e. 10x10 or 20x20 cm respectively also for the antenna design directly relates to the achievable maximum throughput. Antenna design is a key parameter to achieve higher throughput and increase coverage and hence maximize the usage of the 6G-NTN system.

Relevant terminal types are further investigated especially with respect to the antenna analysis for wideband Q/V designs standalone, thus covering a broad enough space matching the

assessed use cases where innovative antenna design can lead to improved terminal performance for 6G NTN.

The assessment and studies shall be conducted for the different acceptable dimensions i.e. 10x10cm and 20x20cm focusing first on Q/V band with maximum dimension.

At a later stage, the analysis shall be performed for the smaller dimension as well, and potentially also for the C band.

2.3 TRANSLATION INTO INVESTIGATION SCOPE

As shown by the analysis performed above, there are mainly 2 device types. The adaptation to the use case scenarios referenced in D2.2 and the UE types named in D2.3 is done via the way of implementation.

These 2 device types have the following characteristics:

Terminal 1 narrowband sub-6GHz (S and L band partially C band), design is common with mobile terminals used for terrestrial communication or the terminal is often a dual-use having full alignment in design. Using state-of-the-art is key for distribution and availability for 6G-NTN communication terminals when being fully integrated into handhelds. Existing handheld terminals need small adaptations for frequency range for NTN but in general frequency range is feasible as being part of the sub-6GHz frequency range. The increased performance and throughput for 6G-NTN for these devices will mainly come, compared to state-of-the art systems, from other systems and design benefits of the 6G-NTN or from improved antenna performance in C band (which, as was already mentioned, will be studied in a later stage).

Terminal 2, wideband and ultra-wideband communication needs achieving multiple 125/250MBits of throughput. Special reference is made here for the performance requirements in D2.3, especially STR-PERF-08 (§4.3.4) in which we very generally state "The 6G-NTN system SHALL be able to serve USAT UE with the performance specified in Table 10 via User Traffic Profile UTP2". Traffic Profile UTP2 is, exhibiting experienced user data rate of 250/125 Mbps. Terminal will operate in mainly Q/V bands. In general, the used frequency range and hence related front-end is not that different from today's terrestrial terminals operating in 5G FR2. The higher pathloss and attenuation in 6G-NTN needs to be compensated/counteracted mainly by the antenna, as in the area of amplifier design and improvements only moderate improvements can be expected.

Especially terminal type 2 which can further be distinguished by the amplifier to be available and sensible for the various use cases is in the major evaluation field. The required amplifier and modem design concerning processing and throughput is considered to be available. Identified use cases and key performance characteristics as identified in D2.2 and D2.3 correspond with today's state –of-the-art terminal designs.

The main gain increase concerning throughput, especially when using Q/V or C band needs to come from new and innovative/improved antenna designs respecting the geometry limitations as analyzed in the user requirements geometry constraints identified in D2.2.

Key performance indicators expressed in D2.3 such as data rate, network performance and throughput are directly related to reception/transmission characteristics, due to similarity and device component constraints only limited gain can be expected from terminal RX/TX modification and hence major performance increase related to the terminal for 6G-NTN needs

to come from antenna design especially in wideband scenarios respecting the UE constraints especially with respect to dimension (small 10x10 and large 20x20cm) as analyzed in the user requirements (D2.2) for the various D2.1 use cases.

The aforementioned focusing of the investigations and studies for the 6G-NTN terminal towards the antenna design and system to be used for 6G-NTN has several reasons and justifications, besides being major impacting factor for throughput and user experience also due to size and weight, bearing highest innovation potential, staying for the other components on state-of-the-art designs and available components is key for allowing classical integrated handhelds for consumers and also stay with more specialized terminals for other use cases ensures sufficient availability at reasonable price being key for 6G-NTN can make it to a mass-market.

Refined investigation scope for the terminal is the antenna design for wideband communication exploiting Q/V and C-band based on deeper survey of today's state-of-the-art and existing NTN requirements (by 3GPP) contained in the next section and new antenna design studies and its design characteristics conducted (chapter 3).

The study on Q/V band antenna performance and new designs will be conducted first based on the larger geometry (20x20cm).

2.4 EXISTING 3GPP REQUIREMENTS FOR NTN UE

In this section, we present a set of existing technical requirements for terminals operating in 3GPP-based non-terrestrial networks. The 3GPP requirements have been defined by 3GPP's RAN4 work group in [32] and refer mainly to the minimum radio frequency (RF) and performance requirements for a UE supporting satellite access operation.

In addition to the 3GPP UE related requirements, we also present requirements defined by ETSI for antennas in fixed radio services operating in frequencies overlapping with the Q/V bands [40].

One of the main advantages of 5G NTN and a target for 6G NTN is to provide service to normal smartphones (handheld) from flying nodes (e.g., LEO satellites). Given that their main use case is to be in coverage from the terrestrial network component, the requirements for smartphones are driven by a different set of documents than [32], namely [37][34][38][39]. Here, we then focus on the specific NTN requirements for terminals.

As mentioned in the previous subsections, , handhelds, in the 6G-NTN project context are expected to be used in the C-band, while very small (VSAT) and ultra small aperture terminals (USAT) are expected to be used in the Q/V bands.

For the mass-market, the form factor and power constraints in a smartphone are expected to be similar in the 6G timeframe. Given the intended use in the C-band, and form factor constraints we expect that such aspects as the antenna design will resemble their counterparts in 5G. This is not true for (mounted) terminals in the Q/V band, as exemplified by the advanced antenna design described in chapter 4].

Given the above, we will focus on presenting the minimum requirements for terminals operating in Q/V bands, with the assumption that the terminal does not have a traditional smartphone form-factor. In other words, the focus is on terminals that can be mounted on vehicles or provide fixed-wireless access, including USAT.

One note about the content that follows is that the requirements are collected from the 3GPP requirements for 5G-NR, since equivalent ones for 6G will be defined later than the time-horizon for 6G-NTN's project conclusion. While possible, we focus on the requirements that

- may be relevant to VSAT/USAT terminals,
- are not dependent on a specific band (e.g., 3GPP band n256),
- are influenced by the choice of antenna design.

This approach is chosen so that for the remainder of the project, we can perform feasibility evaluations that are realistic, with a set of requirements that are likely to resemble their upcoming 6G NTN counterparts.

In a few instances, we list requirements that refer to operation in the FR2-NTN band. While not including the target Q/V bands, these are the highest frequencies considered for 3GPP NTN services so far. In these cases, the requirements are included here as an indication or illustration of what performance or receiver/transmitter characteristics could be expected.

Unless noted, the requirements presented next originate from [32]. In the remainder of this section, we use the term user equipment (UE) to represent both smartphones and access terminals with other form factors.

2.4.1 Bands of interest for the 6G-NTN project

The frequency bands below are considered for research activities in the 6G-NTN project [41], a detailed study on the 6G NTN frequency bands is conducted within D2.5.

2.4.1.1 Q/V bands

The Q/V-bands have been identified as candidate for use in the service link as part of 6G NTN, with the following frequency ranges for both NGSO and GSO satellite services:

- Downlink: 37.5 – 42.5 GHz (Q-band).
- Uplink: 47.2 – 50.2 GHz and 50.4 – 51.4 GHz (V-band).

2.4.1.2 C band

The C-band is a new NTN frequency band opportunity for direct connectivity to smartphones and cars to be considered for the 6G-NTN project

- Downlink NTN satellite communications could potentially use TN TDD (Time Division Duplex) frequency bands n77 (3,300 – 4,200 MHz) / n78 (3,300 – 3,800 MHz).
- Uplink NTN satellite communications could potentially use the upper frequency spectrum (around 6 GHz) or lower frequency spectrum (e.g., UL n255 or UL n256).

2.4.2 Operating bands and channel arrangement

The channel arrangements presented in this section are based on the operating bands and channel bandwidths defined in [32].

Requirements throughout the RF specifications are in many cases defined separately for different frequency ranges (FR). The frequency ranges in which NTN satellite can operate according to 3GPP release 18 specifications are identified as described in Table 2.

As specified in [32], the bands in Table 2 only support frequency division duplexing (FDD) operation.

Table 2: Definition of NTN frequency ranges

Frequency range designation	Corresponding frequency range
FR1-NTN[1]	410 MHz – 7125 MHz
FR2-NTN[2]	17300 MHz – 30000 MHz
NOTE 1: [NTN bands within this frequency range are regarded as a FR1 band when referenced from other 3GPP specifications.] NOTE 2: [NTN bands within this frequency range are regarded as a FR2 band when referenced from other 3GPP specifications.]	

2.4.2.1 Non Terrestrial Network operating bands

Below are current bands that have been designated for FR1-NTN and FR2-NTN.

Table 3 Designated operating bands for FR1-NTN and FR2-NTN

NTN satellite operating band	Uplink (UL) operating band Satellite Access Node receive / UE transmit $F_{UL,low}$ – $F_{UL,high}$	Downlink (DL) operating band Satellite Access Node transmit / UE receive $F_{DL,low}$ – $F_{DL,high}$	Duplex mode
n256	1980 MHz – 2010 MHz	2170 MHz – 2200 MHz	FDD
n255	1626.5 MHz – 1660.5 MHz	1525 MHz – 1559 MHz	FDD
n254	1610 – 1626.5 MHz	2483.5 – 2500 MHz	FDD
n512[1]	27500 MHz - 30000 MHz	17300 MHz - 20200 MHz	FDD
n511[2]	28350 MHz - 30000 MHz	17300 MHz - 20200 MHz	FDD
n510[3]	27500 MHz - 28350 MHz	17300 MHz - 20200 MHz	FDD

NOTE: NTN satellite bands are numbered in descending order from n256.

NOTE 1: This band is applicable in the countries subject to CEPT ECC Decision(05)01 and ECC Decision (13)01.

NOTE 2: This band is applicable in the USA subject to FCC 47 CFR part 25.

NOTE 3: This band is applicable for Earth Station operations in the USA subject to FCC 47 CFR part 25. FCC rules currently do not include ESIM operations in this band (47 CFR 25.202).

Below is a figure describing the designation of the 3GPP specified NTN bands together with the bands that are studied in 6G-NTN.

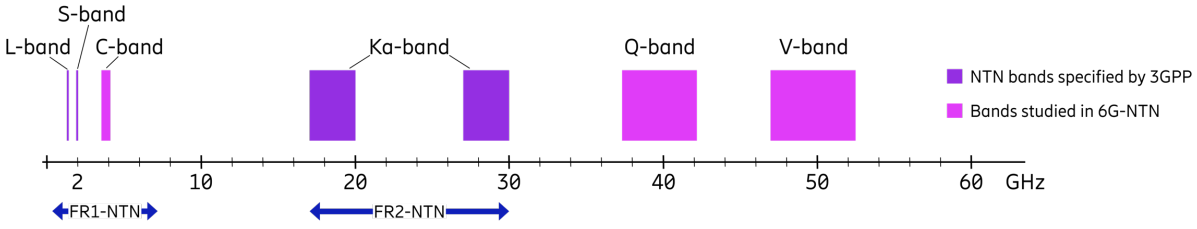

Figure 3. 3GPP specified NTN band together with the bands studied in 6G-NTN

2.4.2.2 Terrestrial Network operating bands

The designation of operating bands for the terrestrial network (TN), defined in [34] is different and listed below for reference. For terrestrial networks, the FR1 frequency supports both FDD and TDD usage.

Table 4: Frequency range designation for TN

Frequency range designation		Corresponding frequency range
FR1		410 MHz – 7125 MHz
FR2	FR2-1	24250 MHz – 52600 MHz
	FR2-2	52600 MHz – 71000 MHz

Details for the definition of bands in the FR2-1 range [34] are listed in *Table 5*.

While the frequencies of interest for 6G-NTN (see Section 2.4.1) are not covered by *Table 4*, they overlap with the definition for TN FR2 according to *Table 5*. Some of the requirements defined in [34] may be applicable to UEs in the Q/V bands, with the caveat that they are specified for TN TDD systems in addition to the parameters in [32] which are specifically tailored toward the satellite use case.

Table 5: Band designation for FR2-1 (TN)

Operating Band	Uplink (UL) operating band BS receive UE transmit	Downlink (DL) operating band BS transmit UE receive	Duplex Mode
	F_{UL_low}[2] – F_{UL_high}[3]	F_{DL_low} – F_{DL_high}	
n257	26500 MHz – 29500 MHz	26500 MHz – 29500 MHz	TDD
n258	24250 MHz – 27500 MHz	24250 MHz – 27500 MHz	TDD
n259	39500 MHz – 43500 MHz	39500 MHz – 43500 MHz	TDD
n260	37000 MHz – 40000 MHz	37000 MHz – 40000 MHz	TDD
n261	27500 MHz – 28350 MHz	27500 MHz – 28350 MHz	TDD
n262	47200 MHz – 48200 MHz	47200 MHz – 48200 MHz	TDD
n263	57000 MHz – 71000 MHz	57000 MHz – 71000 MHz	TDD[1]

NOTE 1: This band is for unlicensed operation and subject to regional and/or country specific regulatory requirements.

NOTE 2: F_{UL_low}, F_{DL_low} indicate the lower limit for the uplink and downlink bands respectively

NOTE 3: F_{UL_high}, F_{DL_high} indicate the upper limit for the uplink and downlink bands respectively

2.4.2.3 UE channel bandwidth

2.4.2.3.1 General

The UE channel bandwidth (BW) supports a single radio frequency (RF) carrier in the uplink or downlink at the UE. From a Satellite Access Node (SAN) perspective, different UE channel bandwidths may be supported within the same spectrum for transmitting to and receiving from UEs connected to the SAN.

From a UE perspective, the UE is configured with one or more bandwidth parts (BWP) / carriers, each with its own UE channel bandwidth. The UE does not need to be aware of the SAN channel bandwidth or how the SAN allocates bandwidth to different UEs.

The placement of the UE channel bandwidth for each UE carrier is flexible but can only be done completely within the SAN channel bandwidth.

The relationship between the channel bandwidth, the guardband and the maximum transmission bandwidth configuration is shown in Figure 4.

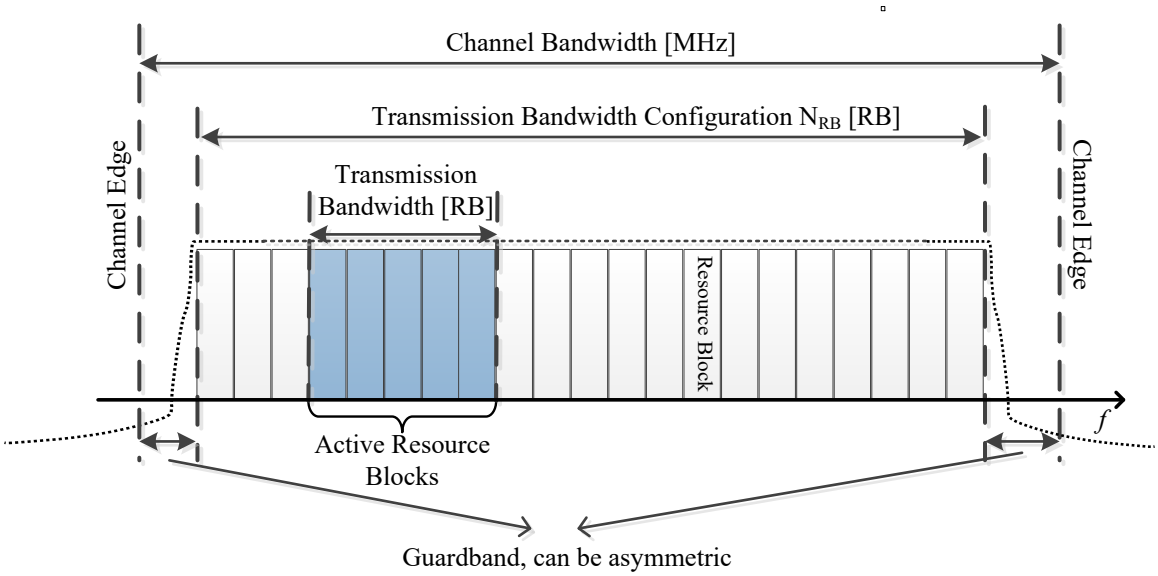

Figure 4: Definition of the channel bandwidth and the maximum transmission bandwidth configuration for one channel

2.4.2.3.2 Maximum transmission bandwidth configuration

The maximum transmission bandwidth configuration is defined in resource blocks (N_{RB}) for each UE channel bandwidth and subcarrier spacing (SCS) in Table 6 for FR1-NTN and Table 7 for FR2-NTN. A resource block is a group of 12 subcarriers with the given subcarrier spacing.

Table 6: Maximum transmission bandwidth configuration NRB for FR1-NTN

SCS (kHz)	5 MHz	10 MHz	15 MHz	20 MHz	30 MHz
	N_{RB}	N_{RB}	N_{RB}	N_{RB}	N_{RB}
15	25	52	79	106	160
30	11	24	38	51	78
60	N/A	11	18	24	38

Table 7: Maximum transmission bandwidth configuration NRB for FR2-NTN

SCS (kHz)	50 MHz	100 MHz	200 MHz	400 MHz
	N_{RB}	N_{RB}	N_{RB}	N_{RB}
60	66	132	264	N/A
120	32	66	132	264

2.4.3 Radiated Transmitter Characteristics

2.4.3.1 General

Unless otherwise stated, the transmitter characteristics are specified over the air (OTA) with a single or multiple transmit chains.

2.4.3.2 Transmitter power

2.4.3.2.1 UE maximum output power

2.4.3.2.1.1 General

The UE classes are specified based on the assumptions of certain UE types with specific device architectures including antenna beam steering types. The requirements are specified for different UE types. And for hybrid beam steering capable UE, which can adjust its antenna(s) or beam(s) in both electronic steering and mechanical steering ways, the applicable requirements should follow either electronic or mechanical beam steering requirements depending on the UE type it declared. The UE types can be found in Table 8 below.

Table 8: Assumptions of UE Types

UE class	UE type	Type description
Fixed VSAT	1	Fixed VSAT communicating with GSO and LEO with mechanical steering antenna.
	2	Fixed VSAT communicating with GSO and LEO with electronic steering antenna.
	3	Fixed VSAT communicating with LEO only with electronic steering antenna.
Mobile VSAT	4	Mobile VSAT communicating with GSO with mechanical steering antenna.
	5	Mobile VSAT communicating with GSO with electronic steering antenna.
Note 1: The UE types are assuming UE has only one antenna beam towards one satellite at a given time in this release. Note 2: The Mobile VSAT communicating with non-GSO is not considered in this release.		

2.4.3.2.1.2 Minimum requirements for Fixed VSAT

The following requirements define the maximum output power radiated by the UE for any transmission bandwidth within the channel bandwidth for non-carrier aggregation (CA) configuration, unless otherwise stated. The period of measurement shall be at least one sub frame (1ms). The minimum output power values for Equivalent Isotropic Radiated Power (EIRP) are found in Table 9. The requirement is verified with the test metric of EIRP (Link=TX beam peak direction, Meas=Link angle).

Table 9: UE minimum peak EIRP for Fixed VSAT

Operating band	UE Type	Min peak EIRP (dBm)
n512, n511, n510	1	70
	2	70
	3	61
Note: Minimum peak EIRP is defined as the lower limit without tolerance.		

The maximum output power values for EIRP are found in Table 10 below.

Table 10: UE maximum output power limits for Fixed VSAT

Operating band	Max EIRP (dBm)
n512, n511, n510	76.2

2.4.3.2.1.3 Minimum requirements for Mobile VSAT

The following requirements define the maximum output power radiated by the UE for any transmission bandwidth within the channel bandwidth for non-CA configuration, unless otherwise stated. The period of measurement shall be at least one sub frame (1ms). The

minimum output power values for EIRP are found in Table 11. The requirement is verified with the test metric of EIRP (Link=TX beam peak direction, Meas=Link angle).

Table 11: UE minimum peak EIRP for Mobile VSAT

Operating band	UE Type	Min peak EIRP (dBm)
n512, n511	4	70
	5	70
Note: Minimum peak EIRP is defined as the lower limit without tolerance.		

The maximum output power values for EIRP are found in Table 12 below.

Table 12: UE maximum output power limits for Mobile VSAT

Operating band	Max EIRP (dBm)
n512, n511	76.2

2.4.3.3 Transmitter signal quality

2.4.3.3.1 Frequency Error

The VSAT UE basic measurement interval of modulated carrier frequency is 1 uplink (UL) slot. The VSAT UE pre-compensates the uplink modulated carrier frequency by the estimated Doppler shift according to 3GPP TS 38.300 [33] clause 16.14.2. The mean value of basic measurements of VSAT UE modulated carrier frequency shall be accurate to within ± 0.1 parts per million (PPM) observed over a period of 1 ms of cumulated measurement intervals compared to ideally pre-compensated reference uplink carrier frequency.

[NOTE: The ideally pre-compensated reference uplink carrier frequency consists of the UL carrier frequency signaled to the VSAT UE by SAN and UL pre-compensated Doppler frequency shift. For the test case, the location of the VSAT UE is explicitly provided to the VSAT UE from the test equipment.]

Requirement will be verified for at least two cases of which one has zero Doppler conditions.

The frequency error is defined as a directional requirement. The requirement is verified in beam locked mode with the test metric of Frequency (Link=TX beam peak direction, Meas=Link angle).

2.4.3.3.2 Transmit modulation quality

The requirements for transmit modulation quality defined in 3GPP TS 38.101-2 [34] clause 6.4.2 except clause 6.4.2.6 shall apply for VSAT UE.

2.4.3.4 Output RF spectrum emissions

2.4.3.4.1 Occupied bandwidth

Occupied bandwidth (OBW) is defined as the bandwidth containing 99 % of the total integrated mean power of the transmitted spectrum on the assigned channel. The occupied bandwidth for all transmission bandwidth configurations (Resources Blocks) shall be less than the channel bandwidth specified in Table 13.

The occupied bandwidth is defined as a directional requirement. The requirement is verified in beam locked mode with the test metric of OBW (Link=TX beam peak direction, Meas=Link angle).

Table 13: Occupied channel bandwidth

	Occupied channel bandwidth / Channel bandwidth			
	50 MHz	**100 MHz**	**200 MHz**	**400 MHz**
Channel bandwidth (MHz)	50	100	200	400

2.4.3.4.2 Out of Band Emissions

2.4.3.4.2.1 General

The out of band (OoB) emissions are unwanted emissions immediately outside the assigned channel bandwidth resulting from the modulation process and non-linearity in the transmitter but excluding spurious emissions (SE). This OoB emission limit is specified in terms of a spectrum emission mask and an adjacent channel leakage power ratio. Additional requirements to protect specific bands are also considered.

The requirements in subsection 2.4.3.4.2.2 only apply when both UL and DL of a VSAT UE are configured for single component carrier (CC) operation, and they are of the same bandwidth.

2.4.3.4.2.2 Spectrum emission mask

The spectrum emission mask of the VSAT UE applies to frequencies starting from the ± edge of the assigned NR channel bandwidth.

2.4.3.4.2.2.1 General NR spectrum emission mask

The power of any VSAT UE emission shall not exceed the levels specified in

Table 14 for the specified channel bandwidth. The requirement is verified in beam locked mode with the test metric of total radiated power (TRP) (Link=TX beam peak direction, Meas=TRP grid).

Table 14: General NR spectrum emission mask for NTN-FR2

Frequency offset of measurement filter -3dB point, Δf	Frequency offset of measurement filter centre frequency, f_offset	Basic limits (dBm)	Measurement bandwidth
0 MHz ≤ Δf < 2× BW	0.5 MHz ≤ f_offset < 2× BW + 0.5 MHz	$max\left(SE\ limit, \mathrm{P}_{\mathrm{rated,UE}} - 10\log10(\mathrm{BW}) - 40 \times log10\left(\frac{f\_offset - 0.5}{BW} \times 2 + 1\right)\right) dBm$	1 MHz
NOTE 1: $P_{rated,UE}$ is TRP for VSAT UE; NOTE 2: Transmission BW is in the unit of MHz; NOTE 3: SE limit 11dBm/1MHz is spurious emission limit specified in spurious emission clause 2.4.3.4.4, and is converted from the SE limit requirement defined on 4 kHz to a value defined over 1 MHz; NOTE 4: Power Spectrum Density (PSD) attenuation as in [35], Annex 5, OoB domain emission limits for earth stations.			

2.4.3.4.3 Adjacent channel leakage ratio

Adjacent Channel Leakage power Ratio (ACLR) is the ratio of the filtered mean power centred on the assigned channel frequency to the filtered mean power centred on an adjacent channel frequency. ACLR requirement is specified for a scenario in which adjacent carrier is another NR channel.

NR Adjacent Channel Leakage power Ratio (NR_{ACLR}) is the ratio of the filtered mean power centred on the assigned channel frequency to the filtered mean power centred on an adjacent channel frequency at nominal channel spacing. The assigned NR channel power and adjacent NR channel power are measured with rectangular filters with measurement bandwidths specified in Table 15 for FR2-NTN.

If the measured adjacent channel power is greater than –35 dBm then the NR_{ACLR} shall be higher than the value specified in Table 154. The requirement is verified in beam locked mode with the test metric of TRP (Link=TX beam peak direction, Meas=TRP grid).

Table 15: General requirements for NR_{ACLR} for FR2-NTN

	Channel bandwidth / NR_{ACLR} / Measurement bandwidth			
	50 MHz	**100 MHz**	**200 MHz**	**400 MHz**
NR_{ACLR} for band n512, n511, n510	(14) dB	(14) dB	(14) dB	(14) dB
NR channel measurement bandwidth (MHz)	47.58	95.16	190.20	380.28
Adjacent channel center frequency offset (MHz)	+50 / -50	+100 / -100	+200 / -200	+400 / -400

2.4.3.4.4 Spurious Emissions

2.4.3.4.4.1 General

Spurious emissions are emissions which are caused by unwanted transmitter effects such as harmonics emission, parasitic emissions, intermodulation products and frequency conversion products, but exclude OoB emissions unless otherwise stated. The spurious emission limits are specified in terms of general requirements in line with SM.329 [36] and NR operating band requirement to address UE co-existence. Spurious emissions are measured as TRP.

To improve measurement accuracy, sensitivity and efficiency, the resolution bandwidth may be smaller than the measurement bandwidth. When the resolution bandwidth is smaller than the measurement bandwidth, the result should be integrated over the measurement bandwidth in order to obtain the equivalent noise bandwidth of the measurement bandwidth.

Unless otherwise stated, the spurious emission limits apply for the frequency ranges that are more than F_{OOB} (MHz) in Table 16 starting from the edge of the assigned NR channel bandwidth. The spurious emission limits in Table 17 apply for all transmitter band configurations (NRB) and channel bandwidths. The requirement is verified in beam locked mode with the test metric of TRP (Link=TX beam peak direction, Meas=TRP grid).

NOTE: For measurement conditions at the edge of each frequency range, the lowest frequency of the measurement position in each frequency range should be set at the lowest boundary of the frequency range plus MBW/2. The highest frequency of the measurement position in each frequency range should be set at the highest boundary of the frequency range minus MBW/2. MBW denotes the measurement bandwidth defined for the protected band.

Table 16: Boundary between NR OoB and spurious emission domain

Channel bandwidth	50 MHz	100 MHz	200 MHz	400 MHz
OOB boundary F_{OOB} (MHz)	100	200	400	800

Table 17: Spurious emissions limits

Frequency Range	Maximum Level	Measurement bandwidth
30 MHz ≤ f ≤ 2nd harmonic of the upper frequency edge of the UL operating band in GHz	-13 dBm	4 kHz

2.4.4 Radiated Receiver Characteristics

2.4.4.1 General

Unless otherwise stated, the receiver characteristics are specified over the air (OTA) at the Radiated Interface Boundary (RIB) for Ka bands fixed and mobile VSAT. The reference effective isotropic sensitivity (EIS), wanted signals and interference are defined assuming a 0 dBi reference antenna located at the center of the quiet zone.

2.4.4.2 Polarization characteristics

The minimum requirements on the receiver characteristics apply under one polarization.

2.4.4.3 OTA reference sensitivity level

2.4.4.3.1 General

The OTA reference sensitivity (REFSENS) requirement is a *directional requirement* and is intended to ensure the minimum OTA reference sensitivity level at the centre of the quiet zone in the receive (RX) beam peak direction. The OTA reference sensitivity power level $EIS_{REFSENS}$ is the minimum mean power received over the air at the RIB, at which the throughput shall meet or exceed the requirements for a specified reference measurement channel.

2.4.4.3.2 Minimum requirement for mobile VSAT

The throughput shall be ≥ 95 % of the maximum throughput of the reference measurement channels as [specified in Annexes A.2.3.2 and A.3.3.2 of [32] (with one sided dynamic orthogonal frequency-division multiple-access (OFDMA) Channel Noise Generator (OCNG) Pattern OP.1 Frequency Division Duplexing (FDD) for the downlink (DL)-signal as described in Annex A.5.2.1) with peak reference sensitivity specified in Table 187]. The requirement is verified with the test metric of EIS (Link=RX beam peak direction, Meas=Link Angle).

Table 18: OTA reference sensitivity requirement for mobile VSAT

Operating band	***VSAT channel bandwidth* (MHz)**	**UL/DL RB allocation**	**OTA reference sensitivity level, $EIS_{REFSENS}$ (dBm)**
n512, n511	50, 100, 200, 400	Full RB allocation N_{RB} as specified in clause 2.4.2.3.2	$EIS_{REFSENS\_50MHz} + 10log_{10}(N_{RB} \times SCS \times 12 / factor)$ (NOTE 1)
NOTE 1: The "factor" represents the normalized factor to scale EIS for different (Channel bandwidth, SCS) configurations. The value of factor is 66 RBs x 60 kHz SCS x 12, i.e. 47520 kHz.			

For Mobile VSAT communication with GSO, $EIS_{REFSENS\_50MHz}$ is [-126.8] dBm.

2.4.4.3.3 Minimum requirement for fixed VSAT

The throughput shall be ≥ 95 % of the maximum throughput of the reference measurement channels as [specified in Annexes A.2.3.2 and A.3.3.2 of [32] (with one sided dynamic OCNG Pattern OP.1 FDD for the DL-signal as described in Annex A.5.2.1) with peak reference sensitivity specified in Table 18 The requirement is verified with the test metric of EIS (Link=RX beam peak direction, Meas=Link Angle).

Table 19: OTA reference sensitivity requirement for fixed VSAT

Operating band	***VSAT channel bandwidth* (MHz)**	**UL/DL RB allocation**	**OTA reference sensitivity level, $EIS_{REFSENS}$ (dBm)**
n512, n511, n510	50, 100, 200, 400	Full RB allocation N_{RB} as specified in clause 2.4.2.3.2	$EIS_{REFSENS\_50MHz} + 10log_{10}(N_{RB} \times SCS \times 12 / factor)$ (NOTE 1)
NOTE 1: The "factor" represents the normalized factor to scale EIS for different (Channel bandwidth, SCS) configurations. The value of factor is 66 RBs x 60 kHz SCS x 12, i.e. 47520 kHz.			

For fixed VSAT communication with GSO and LEO, $EIS_{REFSENS\_50MHz}$ is [-126.8] dBm.

For fixed VSAT communication with LEO only, $EIS_{REFSENS\_50MHz}$ is [-115.6] dBm.

2.4.5 fixed radio service requirements applicable for antennas in the Q/V band

Another source of requirements applicable to terminals operating in the Q/V bands is the ETSI specification EN 302 217-4 [40]. It covers fixed radio services for frequencies in the Q/V band and describes requirements for antennas in frequency ranges between 1 GHz and 86 GHz.

For co-existence and general spectrum compliancy, the radiation pattern envelope (RPE) for an antenna is an important parameter. It provides, e.g., the requirement on allowed side lobe level in azimuth degrees from the main lobe. The RPE for frequencies between 30 and 47 GHz is illustrated in Figure 5 below, adapted from [40].

The fixed radio services use FDD, so the duplexing distances that are specified in [40] for the bands coinciding with the 6G-NTN Q/V could also be used as an input for future analysis of the UE antenna requirement specification (See chapter 4).

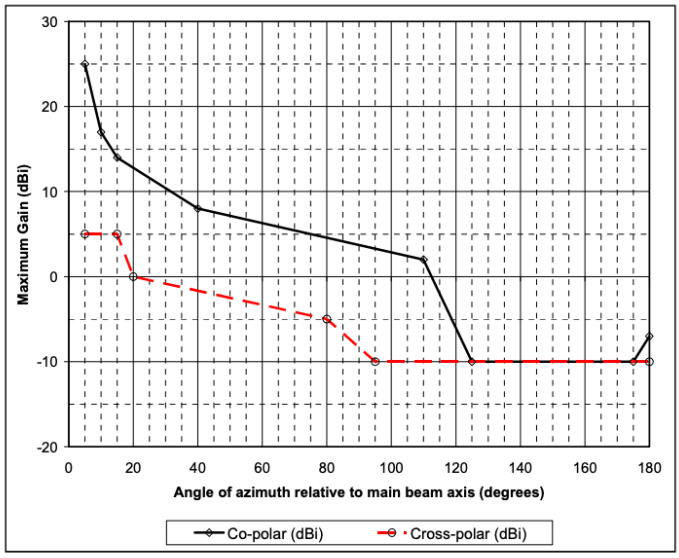

Angle (°)	Co-polar (dBi)	Angle (°)	Cross-polar (dBi)
5	25	5	5
10	17	15	5
15	14	20	0
40	8	80	-5
110	2	95	-10
125	-10	180	-10
175	-10		
180	-7		

Figure 5: RPEs for class 1 antennas in the frequency range from 30 to 47 GHz

It should also be observed that in the 6G-NTN deliverable 4.4 [41] there are assumptions given for the radiation pattern when simulating interferences into other systems. The requirement put on antennas based on new technologies for the radiation pattern could as a first approach, be required to stay within the limits for the antenna radiation pattern used in the co-existence simulations in [41].

3 ANTENNA TECHNOLOGY SURVEY IN C AND Q/V BAND

3.1 INTRODUCTION AND INVESTIGATION SCOPE FOR ANTENNAS

The aim of this chapter is to provide a survey on Q/V and C-Band antenna technologies, focused on moving terminal applications, nicknamed as Satellite On-The-Move (SOTM), Earth Station in Motion (ESIM) and/or Earth Station on Moving Platform (ESOMP),and considering the requirements already derived in previous section for mounted devices, which are the main object of study in 6G-NTN project. The critical join analysis of the State-of-the-Art technologies and the terminal requirements allows identifying promising solutions determining short and mid-term research paths. Therefore, the next two sections provide an antenna technology survey and a critical analysis of potential solutions for both Q/V and C-band, taking into account the specific requirements of identified 6G-NTN terminal types.

Let us remark that for satellites terminals, the term “antenna” is often not limited to the device radiating/receiving the intended signals but it includes everything between the modem output/input, typically at L-band, and the radiating elements themselves. Since satellite systems typically operate in frequency division duplex (FDD) scheme, these may include two different antenna apertures containing the radiating mechanisms for Tx and Rx as well as their corresponding up and down conversion circuits. In addition, an Antenna Control Unit (ACU) featuring a more or less sophisticated inertial system is responsible for controlling the antenna pointing in close collaboration with the modem. This modem-antenna interface is often standardized using OpenAMIP [1] solution. The analysis performed here will be focused on the radiating apertures, since for the rest of components, the use of the Q/V band or the specific 6G-NTN requirements does not imply significant changes.

3.2 ANTENNA TECHNOLOGY SURVEY IN Q/V BAND

A quick analysis of the state-of-the-art reveals that there is only one pre-commercial SOTM terminal in Q/V band provided by ThinKom. Remarkably, it implements a passive mechanical steering solution, based on the ThinKom patented Variable Inclination Continuous Transverse Stub (VICTS) technology [3]. As depicted in Figure 6, it consists of two panels placed one on top of the other supporting a parallel plate waveguide transmission. The lower panel implements parallel plate mode feeding lines, and the upper transverse stubs that create a leaky wave that is responsible of the radiation of a narrow pencil beam. By controlling the relative rotation between both panels, the beam can be steered in both azimuth and elevation angles.

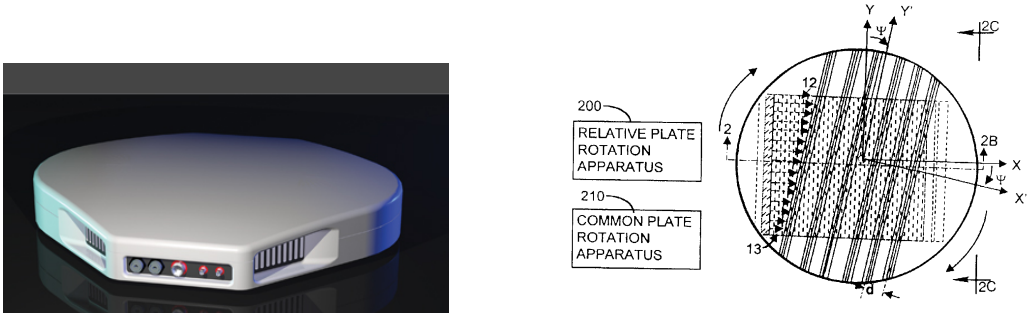

Figure 6: ThinKom pre-commercial Q/V- band terminal. Left: Terminal picture from [2]; right: VICTS technology from [3]

The fact that the first pre-commercial product is based on mechanical steering may be just a coincidence, obeying the ThinKom strategy to be the first announcing a product in the market, but it exemplifies the challenges of developing a cost and power efficient low-profile antenna with electronic steering at millimetre wave ranges. It is foreseen that once the market demands them (note that nowadays Q/V are mostly considered for the feeder link), more players will develop antenna terminals in different technologies, as is the case today for Ka and Ku bands. Indeed, the jump between Ka and Q/V is not that high, so it could be envisaged that the same technologies will be used and adapted to the Q/V range. Therefore, we analyse next the evolution of SOTM antenna terminals in commercial Ku/Ka bands.

Firstly, let us remark that the antenna has been traditionally the main barrier for the massive spread of SOTM terminals. It represents 90% of the terminal cost [4], and their size, power consumption and weight represent also challenges for their deployment on smaller platforms like cars. The move to LEO orbits opens new opportunities since lower pathloss require reduced antenna sizes, so reduced costs. Indeed, Starlink terminals can be seen as a massive deployment of beam scanning antennas, though in this case they are fixed terminal, not SOTM ones. Wide reviews on antenna technologies for SOTM [5], LEO terminals [6], beam steering solution for satellite communications (SATCOM) and 5G [7] or just for 5G [8] have been already published.

Initial SOTM terminals relayed on mechanically steered parabolic reflectors, resulting in heavy and bulky systems not suitable for smaller platforms. Nowadays they still have applications in large platforms like vessels. The need for more aerodynamic low-profile solutions went through the use of modified reflectors to the implementation of single or multiple rectangular panels. Passive mechanical steering, as already explained for the VICTS case, is still a suitable technology when considering cost and power efficiency. A review on recent passive steering solutions is presented in [4], which includes the discussion of low profile near-field meta-steering antenna systems. They can be seen as an extension of the VICTS concept in which a low layer excites an upper layer consisting of a metasurface creating a radiating leaky wave mode. The mechanical interaction between the two layers controls the beam steering. In that regard, Figure 7evolution of mechanically steered antennas.

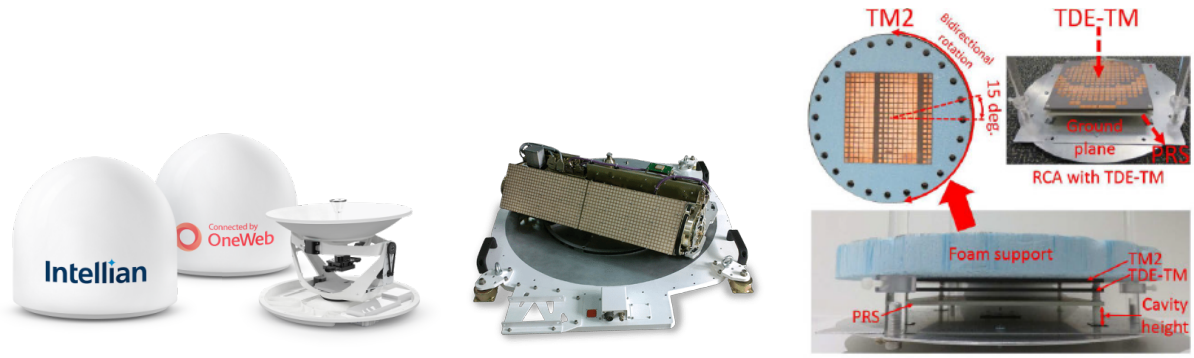

Figure 7: Mechanically steered technology examples. Left: parabolic reflector from [9]); center: flat rectangular panel (from [10]); and right: near-field meta-steering (from [4])

Beam steering reconfiguration rates in mechanically steered parabolic reflectors were in the order of seconds, so the need for fast steering motivated the use of electronic steering solutions. Although initially hybrid systems providing electronic elevation steering and mechanical azimuth steering were issued, nowadays full electronic steering is a reality. Indeed, it experienced a huge progression in the last decade, driven by the needs of both SATCOM and 5G applications, and relying in technological improvements in integrated circuits (IC) and metasurface technologies. Three main steering solutions have been developed: array-based, reflector/lens-based and leaky-wave (metasurface) based. They are further discussed next.

Array-based electronic steering

Electronic steering with array-based antennas has been demonstrated with multiple configurations: tile and brick, digital, analogue and hybrid beamforming, for analogue it has been implemented in RF, intermediate frequency (IF) or local oscillator (LO). For hybrid, partially connected and fully connected solutions have been investigated [7]. For SOTM terminals, the major trend is the tile configuration with analog beamforming at RF. Phasor, now Hanwha-Phasor [11], was one of the pioneering companies demonstrating this technology in a commercial product, as shown in Figure 8. Nowadays, there is a large set of companies using this technology in Ku and Ka bands (e.g., ViaSat, Rockwell Collins, Qest, OneWeb, SpaceX, Boeing, Coxsat, etc.). The main enablers for this solution are the multi-channel beamformer IC and the printed circuit board (PCB) advancements. Specifically, beamformer ICs typically implement amplification (low noise amplifier or power amplifier) and phase and magnitude control for beam steering, for dual polarization and for multiple elements from 4 to 16. This provides the required level of integration for the tile configuration, placing the IC underneath the set 4 or 16 array module. The combination of multiple modules permits realizing large antenna apertures. Several companies like Renesas, Analog Devices or Anokiwave offer Commercial off-the-shelf (COTS) beamformer IC that can be used by system integrators to realize their own antenna solutions. The drawbacks of analog beamforming include the large feeding networks required that imply significant losses, the single-beam operation, and the beam squint in large apertures. All of them can addressed by using digital or hybrid beamforming. Digital beamforming has been demonstrated by Satixfy [12], which developed their own application-specific integrated circuit (ASIC) suitable for given antenna configurations. In the case of hybrid-beamforming, the partially connected solution in which each antenna element is only connected to on RF chain is the preferred choice due to the large apertures. Note that a full-connected solution would require having large combining networks for each antenna element, significantly increasing losses. Losses in feeding networks can be overcome by amplifiers, but it not only worsens the thermal management of the antenna but also the power consumption, which is already a limiting factor in some moving platforms.

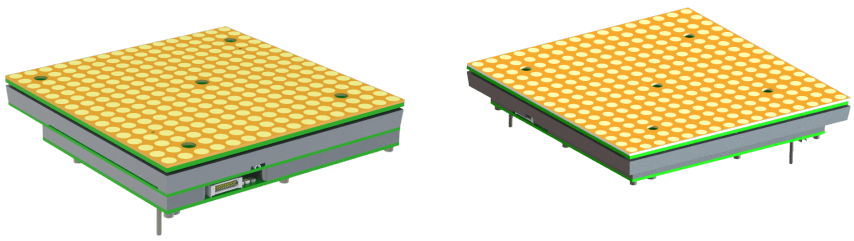

Figure 8: Tx (left) and Rx (right) apertures for Hanwha-Phasor analog RF beamformer antenna

The move to Q/V bands would increase the integration level required, and complicate the thermal management due to the denser element distribution. Still, arrays at 40 GHz have been designed for 5G [7], and it is expected that solution for SATCOM will come if the market demands them.

Reflector/lens-based electronic steering

A potential alternative in order to get rid of the large losses in array feeding networks is the use of spatial feeding configurations of transmit/reflectarrays [13] . In this case, a single feed or a very small array illuminates a reflector or lens surface made of phase shifting reflecting/transmitting elements. Therefore, the beam steering is performed in the spatially illuminated lens/reflector surface and there is no need for feeding networks. However, this

solution requires having the distanced between the feed and the lens/reflector surface similar to the lens/reflector diameter resulting in high profile antennas. They can be reduced by the use of folded reflect array configurations but still the profile is no low enough to be considered as a planar antenna (e.g., [14]).

Leaky-wave/metasurface-based electronic steering

To get rid of large feeding networks and keep low profile configurations, the alternative is to illuminate a metasurface through a parallel plate waveguide mode or a surface wave (metasurface antennas) or a Fabry-Perot cavity (Fabry Perot antennas (FPA)). The metasurface illumination excites a leaky-wave forming the radiation beam at the antenna far-field. This process can be also explained by holographic theory [15]. Leaky-wave antennas inherently scan their beams with the change in frequency, so fixed frequency scanning requires changing the surface impedance of each metasurface unit cell. For metasurface antennas, typically the reconfiguration has been obtained through varactor diodes of liquid-crystal (LC). It must be noted that the size of the metasurface unit cells need to be well below the wavelength, increasing the number of unit cells with respect to array-based systems where half-wavelength is enough. However, the use of simple varactors or LC still provides important power and cost improvements with respect to active arrays. Metasurface antennas has been demonstrated for SOTM applications using LC by Kymeta [16] or for 5G applications using varactor diodes by Pivotal [17], depicted in Figure 9 . Remarkably, Kymeta solution interleaved transmits and receive unit cells on the same metasurface realizing a shared Tx/Rx aperture [7]. For FPA, beam steering at mm-wave has been demonstrated using beam switching with a focal -plane array instead of a single feed element [18]-[19]. In lower frequencies varactor, and PIN diodes, LC or eval liquid-metal has been used but the achieved beam steering was limited and not covering 360º in azimuth and 50º in elevation.

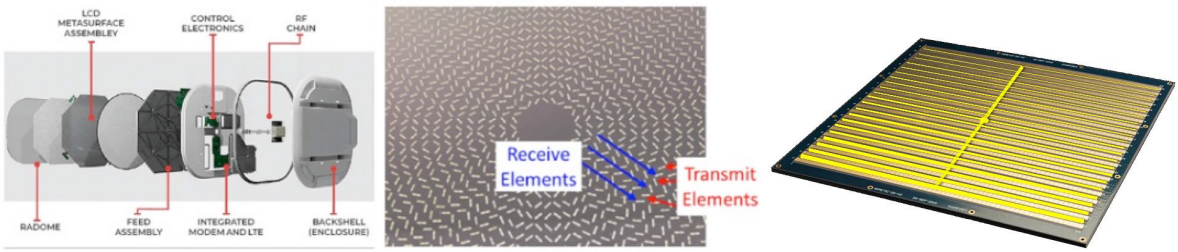

Figure 9: Commercial metasurface antennas. Left: Kymeta from [7]; right: Pivotal from [17]

In this case, moving to Q/V band would again imply a denser grid of unit cells, increasing the number of reconfigurable elements.

Hybrid solutions

Other companies developed terminal antennas using a combination of the aforementioned technologies. This is the case of Isotropic systems, now All. Space, which uses an array of lenses illuminated by focal-plane arrays. The beam steering is achieved by exciting different elements in each focal-plane array. Shared Tx-Rx and multibeam operation is supported by exciting more than one element in each focal-plane array at the same time. Alcan systems is another example, realizing a phased array antenna with LC distributed phase shifters underneath of the radiating elements, providing improvements in terms of power consumption, thermal managements and cost with respect to IC-based phased arrays.

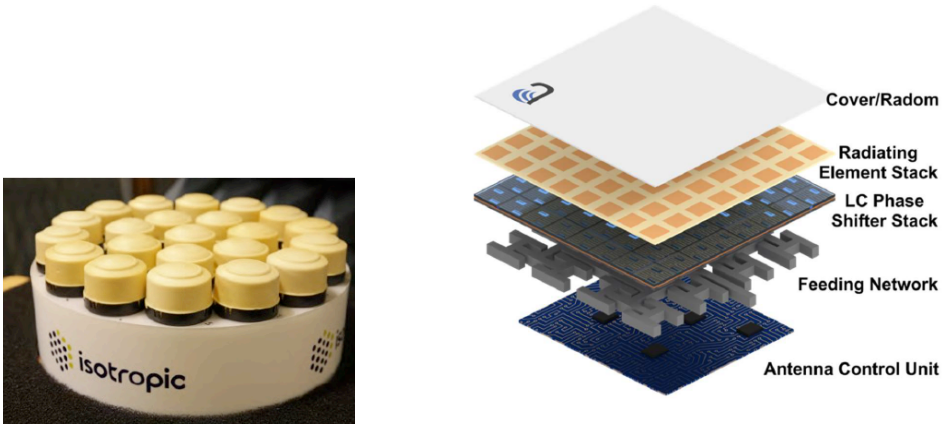

Figure 10: Hybrid commercial metasurface antennas. Left: All.Space array of lenses from [22]; right: Alcan Systems phased array with distributed LC phase shifters from [23]

3.2.1 Critical analysis of Q/V band solutions

The main requirement imposed by the 6G-NTN considered terminals is to have a maximum size of 20x20cm or even 10cmx10cm for the smaller variant. Fixing the antenna size, the antenna design must ensure a minimum aperture efficiency in order to reach a given antenna gain, which was considered to be 32 dBi (20x20cm case) and 28 dBi (10x10cm case) in D3.5. Figure 11 plots the required aperture efficiency for different antenna sizes at 40 GHz. It can be observed that for a 20cmx20cm aperture, the required gain is achieved even for efficiencies as low as 20%. However, considering that the available size needs to be shared by Tx and Rx apertures, the required efficiency increases to 35%. Moreover, if two beam need to be realized in order to implement make-before-break hand overs, the efficiency becomes as high as 70%. The numbers get worser if the smaller variant of 10cm x 10cm is used as a baseline. In this case, only the use of the full aperture allows efficiencies below 50%, whereas with TX -RX and two beams, the required gain is not realizable. Beam steering antennas at Q band may provide rather low aperture efficiencies below 50% so there is a need to exploit efficiently the available area. It can be done through using the same aperture for both Tx and Rx, or even for dual-beam transmission in each direction. As described before, Kymeta or ALL.Space solutions already support shared Tx/Rx aperture, whereas other examples with leaky wave and array solutions can be found in [24] and references therein. Otherwise, link budgets need to be re-analysed if the available area needs to be shared by Tx and Rx and two beams per direction.

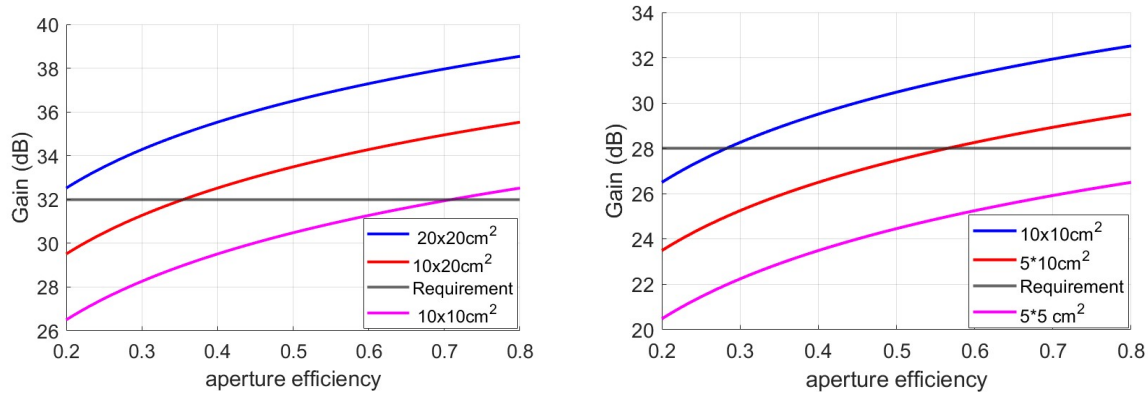

Figure 11: Required aperture efficiencies for different antenna sizes: left 20cmx20cm baseline; right 10cm x10 cm baseline [24]

Array solutions provide accurate control on the phase and amplitude of each array element, and so the best radiation pattern control. However, at this technological stage, their implementation at Q/V present almost unaffordable challenges. First, they need to rely on beamformer IC driving multiple elements and performing both amplification and phase-amplitude variation. These IC will most likely be available in the next future when the use of Q/V band for user link is targeted by the market, but right now there is no availability. Therefore, the implementation of array-based antennas is mostly shifted to the development of highly integrated beamformer ICs. In addition, for an array of 20cmx20cm, more than 2000 elements would be required considering a separation between elements slightly larger than half-wavelength, to avoid the appearance of grating lobes. Hence, large feeding networks would represent another issue to deal with.

Bearing this in mind, leaky-wave antennas are identified as a more suitable solution. Besides the low profile, they provide lower costs and low power consumptions at the price of reduced radiation pattern control, since unit cells are fed from travelling waves that do not permit an exact amplitude control. In the case of metasurface antennas, these unit cells typically have subwavelength sizes ranging between λ/6-λ/8 [25]. As a result, a 20cmx20xm aperture would require tenths of thousands of reconfigurable unit cells, which may be only feasible considering LC technology as in LCD TV monitors. Fabry-Perot architectures may allow alleviating this issue by using larger unit cells, enabling the use of varactor diodes for reconfigurations, which constitute not only a more mature solution but also provide faster beam-steering reconfiguration.

In conclusion, leaky-wave beam steering antennas based on Fabry-Perot excitation and varactor diodes for beam steering reconfiguration seem to be a priori a suitable solution to be further developed in 6G-NTN. In a longer term, the implementation of shared Tx-Rx apertures and dual-beam operation will be also of high interest to make the most efficient use of the available area.

3.3 CRITICAL ANALYSIS OF C BAND SOLUTIONS

C-band has been traditionally used for satellite broadcast or communications, and still have special significance in certain regions due to its lower losses in case of rain and bad weather conditions. In these cases, the considered terminals where VSATS equipped with rather bulky parabolic reflectors. 6G-NTN targets a different use case based on the transmission to/from a vLEO satellite to a handheld terminal or a mobile platform terminal like a drone or a car. Antennas for handheld terminals are well covered by state-of-the-art technology and are not discussed here. Similarly, the set of identified requirements for the mobile platform case, namely a frequency of operation of 3.4 GHz (Rx) and 3.9 GHz (Tx), gain of 0 dBi and bandwidth of 100 MHz (see D3.5), do not require any specific advance over the state-of-the-art. However, depending on the size constraints, the placement location on the platforms and the targeted type of connectivity (only NTN or dual TN-NTN), not so standardized antenna solution would be required. We next discuss four different use cases:

1. **Available area for C-band of 20 cm x 20 cm (10 cm x 10 cm) and NTN only connectivity**

For this case we consider that the available areas discussed previously for the Q/V band are here available only for C-band. In addition, the antenna, needs to connect only with NTN platforms with a minimum elevation of 40º, as considered in D3.5. In these conditions a simple microstrip patch antenna would satisfy all requirements. It may occupy less than 4 cm x 4 cm and require a ground plane around 13.6 cm x 13. 6 cm. So two elements, one for transmission and the other for reception can be easily deployed for both 20 cm x 20 cm and 10 cm x 10 cm

cases. They would provide gains in the range from 5 dBi to 8 dBi and 3dBi to 0dBi at low elevation angle, representing a large improvement on the link budget margin with respect to the requirement of 0 dBi at low elevation angle. They are considered to be placed in a horizontal surface such as the roof of a car, covering the upper half hemisphere with a -3 dB beamwidth around 90º. For the 20 cm x 20 cm case, it may be even possible to include two arrays of 2x2 elements, increasing the gain in 4-5 dB (taking into account implementation losses), but requiring a beam steering solution due to a lower beamwidth. Note that for the 10 cm x 10 cm case, the ground plane size is not an issue, the car rooftop can be used as a ground plane or in the drone case, a reduced ground plane of 10 cm x 10 cm would just imply a slight gain reduction but also would bring a wider beamwidth for a better coverage. In any case, circular polarization can be easily used by exciting two ports with 90º phase difference or by cutting diagonal corners or slits in each patch. A review of compact microstrip patches can be found in [26]

2. **Available area shared with Q/V band of 20 cm x 20 cm (10 cm x 10 cm) and NTN only connectivity**

In this case, we consider that the available areas for deploying the antennas need to be shared by both Q/V and C- band solutions, providing dual-connectivity. Since the analysis of Q/V band solutions revealed that there is a need of fully using the whole available area, the only suitable solution here is to consider multi-functional shared aperture solutions. They represent a research goal that further requires advancements beyond the state-of-the-art. A recent review of multifunctional apertures was provided in [24]. They are of special relevance the included references on dual-frequency shared apertures with high frequency ratios. Some basic solutions are based on using a large structure acting both as a patch for the lower band and as a support for the radiating elements at the higher band like a slot array [27] or a partially reflecting surface forming part of a Fabry-Perot cavity [28]. Interestingly, there are different references proposing solutions including Fabry-Perot cavities, which can be more straightforward used to combine the target C-Band with the already identified Q/V band solution. Note however, that keeping large aperture efficiencies with beam steering functionality at Q/V band and at the same time sharing the aperture with a large C-band patch becomes a research challenge.

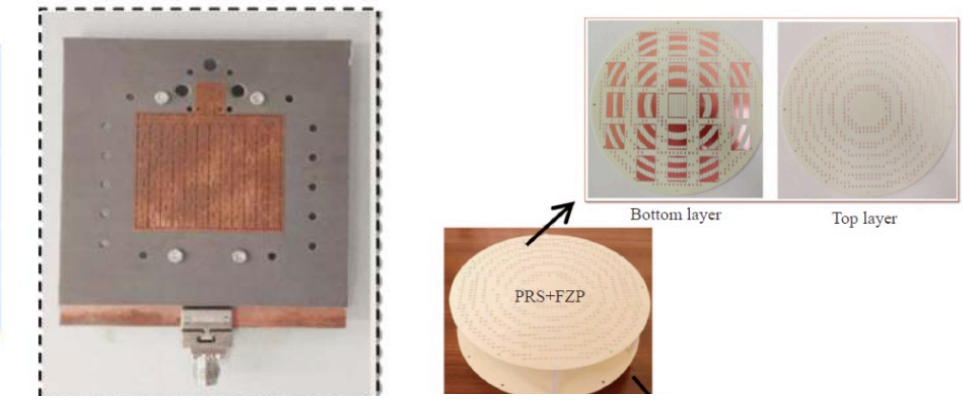

Figure 12: Examples of mm-wave/sub 6GHz dual frequency shared apertures from [24]

In the case of terminals in cars, a potential alternative to shared aperture antennas is to co-locate the C-Band antenna with the antennas of other systems (e.g., Global Positionning System (GPS), frequency/amplitude modulation (FM/AM) radio), which usually are all integrated in a shark fin radome (e.g., Figure 13). The option here would be to resort to miniaturized patch solutions [26] or dielectric loaded helical antenna [29] with low number of turns [30]. The compatibility with the other antennas within the radome would again represent a research challenge.

Figure 13: Shark fin antenna system

3. Dual NTN-TN connectivity

In the case of dual NTN-TN connectivity, the antenna not only needs to point towards the sky supporting a minimum elevation of 40º, but also needs to be able to connect to terrestrial infrastructure. If simultaneous dual-connectivity is targeted, quasi omni-directional patterns are required, which result in reduced directivities and gains, thus not providing link budget margin improvements with respect to the specified 0 dBi gain antennas. For cars, monopole-like structures would permit covering the required half hemisphere while drones need to rely on dipole-like solutions to cover upper and lower hemispheres. Note that both monopoles and dipoles have radiation nulls in their main axis, so using architectures with slanted 45º crossed dipoles would avoid placing a radiation null towards 90 º elevation and at the same time, providing some polarization diversity.

If sequential dual-connectivity is targeted, pattern reconfigurable antennas can be envisaged. For instance, for cars, microstrip patches capable of switching from patch-like to monopole-like patterns can be of interest (e.g. [31]). Note however, that pattern reconfiguration may include some extra losses due to reconfiguration mechanisms, and need to be combined with the size constraints discussed in the previous two points, becoming another open research challenge.

In conclusion, for C-Band, suitable antenna architectures depend on the considered use case. Three open research challenges have been identified: (i) dual frequency Q/V- C-band shared apertures; (ii) Integration of C-band antennas (e.g. patch or helix) in shark fin radomes for cars; and (iii) reconfigurable pattern solutions combined with dual-frequency shared aperture solutions.

4 ANTENNA INVESTIGATION

4.1 INTRODUCTION

The continuous advancement of digitization and technology, including wireless communications and service infrastructure, is reshaping every sector of our economy and society. Expectations are high for 6G to supersede 5G-Advance (5G-A) and user in a new era of enhanced connectivity, pushing the boundaries of communication networks even further [42].

Non-Terrestrial Networks (NTNs) are expected to play a key role in many applications of 6G [43] , facilitating further enhancement of connectivity in rural areas. This is fuelling the need for cutting-edge components for NTNs that can deliver high throughput and low latency services seamlessly integrating with future 6G terrestrial telecommunication networks. These components are expected to enhance system capacity, flexibility, and adaptability to address uncertainties and market changes while also improving system availability, scalability, and resilience. Moreover, they aim to reduce costs and energy consumption [44].

High throughput, increased coverage and ecological trends require designing a low SWaP-C (size, weight, power and cost) components of mobile network like electronically steerable antenna (or commonly called dynamic Metasurface (MTS) antenna-DMA) and reconfigurable intelligent surfaces (RIS)[45], [46], [47], [48]. operating in the new spectrum of the mmWave bands, namely Q-band (37.5 GHz to 42.5 GHz) for receive signals (Rx) and V-band (47.2 GHz to 50.2 GHz) for transmit signals (Tx).

A promising solution for a low cost and low power consumption DMA antenna is antenna based on leaky cavity concept [49], [50].

This antenna relies on wave control inside a cavity rather than wave emission from antenna array. Hence it becomes standard and protocol agnostic, can be compatible with any back-end, and is easily scalable to the required frequency band.

The beamforming of the antenna does not result from the synchronization of many elementary sources such as in phased-array, but rather on the shaping of a wavefield inside a cavity. That is, the same antenna can work for 5G mmWaves or Ka-band satellite communications without need to adapt the radiating elements or the feeding. Moreover it doesn't require the phase shifting elements, individual amplifiers and hence complex and expensive electronics. The beamforming is realized in a passive way (the Metasurface is direct current (DC) active but RF passive). The antenna consumes very little energy to beamform.

Compared to phased arrays, this design approach is much more energy efficient since there are no dissipative circuits or materials to guide the waves, and it can switch beams at the speed of electronics just like active phased arrays. Furthermore, the cavity of the antenna can be made of any shape, meaning that the antenna is perfectly conformable to the surface of an object (vehicule, drones, plane). The Metasurface remind the main part of the DMA leaky cavity antenna and RIS. The technology requires low dissipation in reflection and independent control of the reflected phase for both vertical and horizontal polarizations. The control of the reflected phase is provided by the switching element. In this paper, we introduce the design of the Metasurface for Q- and V-bands exhibiting low dissipation and providing the binary control of the phase of the reflected wave for two polarisations.

4.2 OBJECTIVE

The following table summarizes design and characterization of Q and V band Antenna System for future 6G Non terrestrial Network (NTN) with KPIs:

Table 20: The KPI's Specification of the QV band Antenna System

		Q-Rx size 20cm x 20cm	Q-Tx size 20cm x 20cm
Frequency Range		37.5-42.5 GHz	47.2-50.2 GHz
Beamformer dimension		20cm x 20cmx 3cm ~27x27λ @ 40 GHz	20cm x 20cmx 3cm ~33 x 33 λ @ 50 GHz
Total Efficiency		-14 dB	-14 dB
Gain (Elev 90°)		25.5 dBi	27 dBi
EIRP with BUC 10 Watt		N/A	27 + BUC power i.e. 30 dBW @ 2W BUC
G/T with LNB noise figure of 1.5 dB		~5 dB/K at 90° Elev target: -0.5 dB/K @ 2dB LNB NoiseFigure best: +1 dB/K	N/A
Bandwidth	Total	4 GHz	4 GHz
	Instantaneous (from 0°-60°)	150 MHz	150 MHz
Side Lobe Level		First sidelobe -15 dB typical	First sidelobe -15 dB typical
Scan Angle		ScanLoss (power cos): target: TBD ±70°, 1.4 ±50° best: 1@ ±50	ScanLoss (power cos): target: TBD ±70°, 1.4 ±50° best: 1@ ±50

4.3 ANTENNA COMPONENTS

The full antenna system consists of four main components:

1. Metasurface
2. Antenna Feeder System
3. Antenna Mask
4. Antenna Cavity

4.3.1 Metasurface

The concept of the Metasurface is based on the original design, proposed in [8]. As illustrated by Figure 14, the design can be broken down into three separate parts: a microstrip patch resonator (outlined in a red rectangle), a parasitic resonator (outlined in a green rectangle) and the interconnection region with the active switching component (outlined in a blue rectangle). The phase shift for each pixel of the MTS is controlled by the coupling between the patch and the parasitic element. The resonance frequencies of patch and parasitic elements are defined correspondingly by their electrical length (proportional to physical size) and initially tuned to lay close to each other. The resonance frequency of the parasitic element is fine-tuned by its length. Due to the coupling of the close positioned resonance frequencies, the resonance frequency of the patch resonator depends on and is affected by the resonance of the parasitic element.

To control the operating states of the 1-bit reconfigurable MTS, the parasitic element and the patch are connected through a low-cost active switching component. This component operating as a switch has two states, ON-state and OFF-state. It either allows the current to pass through or isolates its passage, essentially making an electrical connection between the patch and the parasitic or isolating the two. In the general case, different components can be used as active switching element such as PIN diode, micro-electro-mechanical systems (MEMS), photo-diode, VO2, liquid crystal or any other active component which has a switching functionality, meaning it can be put in a conductive or isolating state, ON and OFF state respectively. The selection of the element is dictated by the cost, switching speed, power handling, dissipation, and other requirements. In case of the binary 1-bit control, we deal with OFF and ON states only of the switching component. In the OFF state, the switching component is opened and the phase of the pixel will only be that of the resonating patch. In the ON state the switch is closed and the phase of the pixel will change due to the introduction of the parasitic element of a certain electrical length. During the design process, we are aiming to maximize the reflecting property of the MTS i.e., providing the maximum amplitude of the reflected wave in both states. Perfect binary MTS should provide 0 dB reflection loss, and the 180◦ or π phase shift between the two operating states.

The proposed design ensures the necessary amplitude levels and phase shifts for both TE (horizontal) and TM (vertical) polarization's. As the operational mechanism remains identical for each polarization, the pixel was initially developed to function solely in one polarization. Subsequently, the parasitic element and the active switching component were mirrored along the diagonal axis of the pixel, and optimized to accommodate both polarization's. The subsequent optimization of the design is necessary to minimize the cross-polarization effect, when reflected wave partially converted to the orthogonal polarization. For this reason the patch have truncated corners (see Fig. 1). This also prevents direct shorting to ground via contact with grounding vias. To provide efficient control of the reflected wave and avoid the appearance of the grating lobes, the density of the elements at the Metasurface should not overcome half of the operating wavelength. The size of the designed pixel is 0.5λ × 0.5λ, The pixel was designed using a low-loss substrate, METEROWAVE 8300 from AGC εr = 3, tan δ = 0.0025). The rest of the substrate layers are placed behind the radiofrequency ground and can be fabricated with a conventional FR-4 substrate. The 3D electromagnetic model with floquet boundary conditions was simulated and optimized using a Frequency Domain solver in CST Studio Suite software. The main challenge of the pixel design is to provide a low cost layout suitable for a conventional PCB manufacturing technology.

4.3.1.1 Design and Schematic of the V-Tx Metasurface

1. The Designed unit cell consist of 3 main important elements which could generate the response mentioned in the objectives:
    I. Patch – Main radiating element
    II. Parasitic element – helps generate the phase shift between the two states
    III. Diode – To switch between the two states
2. The phase shift between the two pixel states is obtained by introducing a longer electrical length element, a parasitic element, in the ON state.
3. The parasitic element is shorted directly to a GND via.
4. The main reflector patch, couples to a coupler which is connected to the complementary metal-oxide semiconductor (CMOS) footprint and the parasitic element. The length of the coupler can be adjusted to either increase or decrease the coupling strength.

5. The main reflector patch also has truncated corners, this is done for 2 reasons. Firstly, to make sure that the patch doesn't short directly to ground by touching the vias and second, is to reduce cross coupling.
6. Each switch has 4 GND vias and 1 enable via. The two switches share 1 GND via to save space on the unit cell.
7. Bigger vias were used to reduce the cost per pixel.
8. The detailed dimensions of the whole structure vary depending on the desired frequency band. It will be presented in the following sections.
9. Parameter details:
    I. Substrate heigh = 0.5 mm
    II. Via diameter = 0.25 mm
    III. Via pad diameter = 0.5 mm

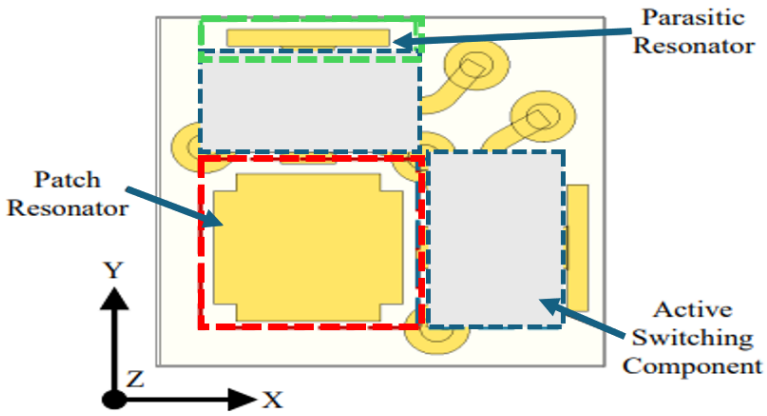

Figure 14: Design of a single unit cell divided into three parts, patch resonator (red), parasitic resonator (green) and active switching component (blue)

4.3.1.2 Simulation Result of V-Tx Unit cell

During the design of a dual polarized pixel, the switch is mirrored with respect to the center of the patch to keep the symmetry for each polarization. During the mirroring process two of the via pads, highlighted below, overlap. Since it wouldn't be feasible to fabricate a design with two vias so close to each other, the design had to be modified to include only one common via.

RESULTS – DISSIPATION AND PHASE DIFFERENCE

CO-POL Dissipation level (S11 Vs Frequency) – 47.2 to 50.2 GHZ: The highest dissipation level is -2.9dB seen at 50.2GHz

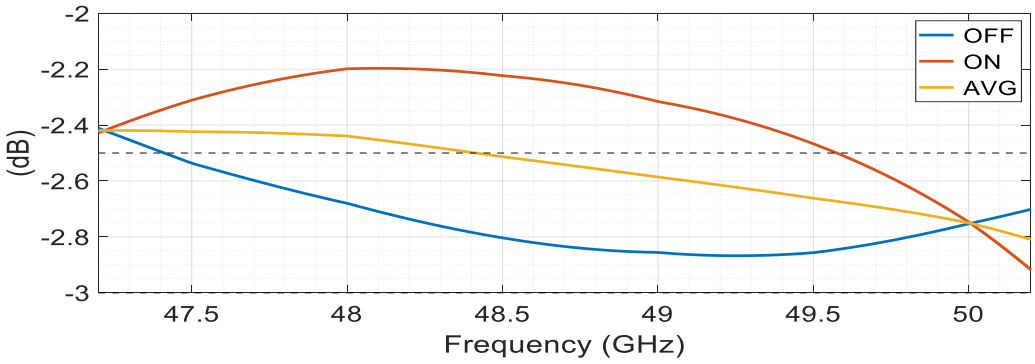

Figure 15: Simulated reflection coefficient versus frequency. The highest dissipation level is -3 dB seen at 50.2 GHZ.

CO-POL Phase difference level – 47.2 to 50.2 GHZ: The phase difference is over 160° across the band

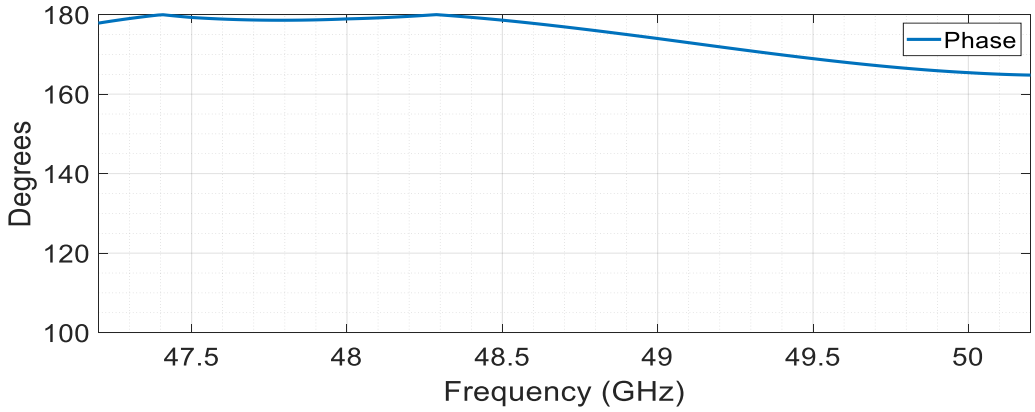

Figure 16 Simulated Phase difference versus frequency across the frequency band of Interest

CO-POL Dissipation level (S11 Vs Frequency) – 40 to 56 GHZ: The highest dissipation level is -2.9dB seen at 50.2GHz

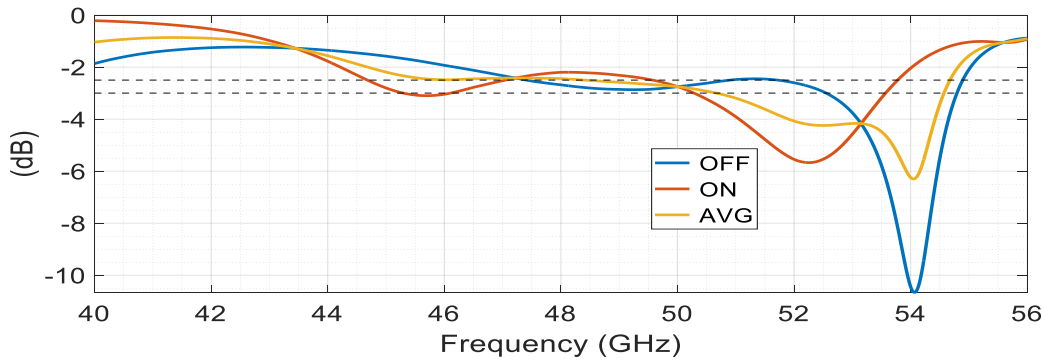

Figure 17: Dissipation versus. Frequency for wide frequency range

CO-POL Phase difference level – 40 to 56 GHZ: The phase difference is over 160° across the band

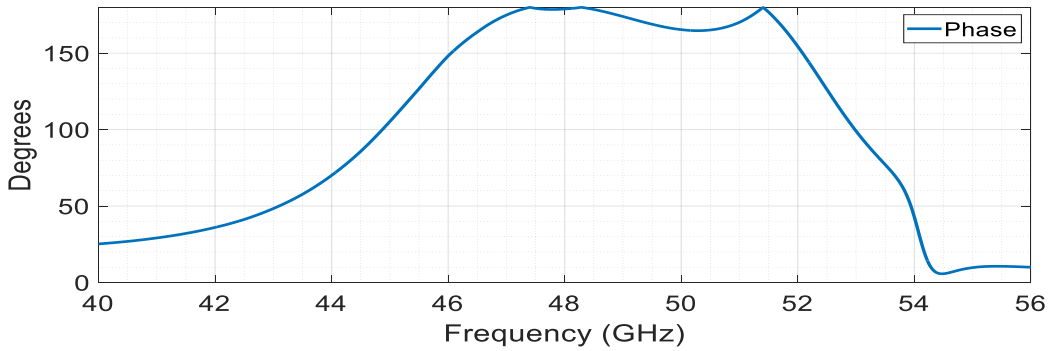

Figure 18: Phase difference versus Frequency

Cross-POL Dissipation level (S11 Vs Frequency) – 40 to 56 GHZ: The X-pol levels in most of the frequency range is below -10 dB.

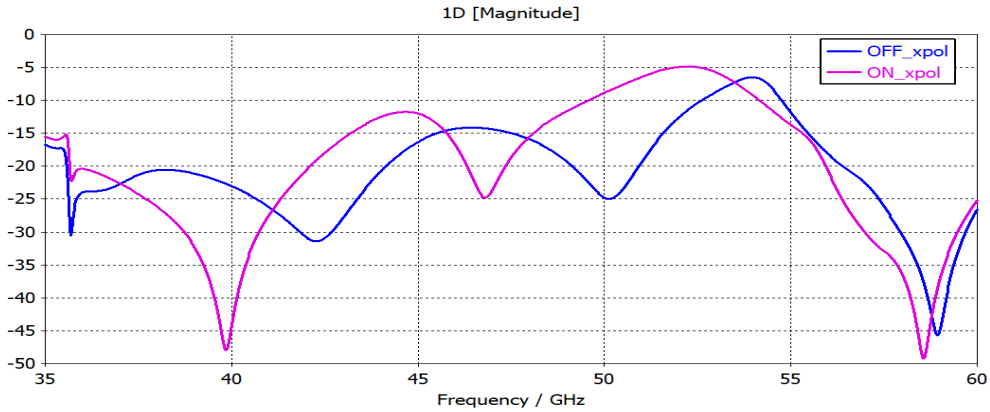

Figure 19: Simulated Cross polarization Dissipation versus Frequency

The simulation results show better than −3 dB and more than 160◦ phase difference in the band of interest (47.2− 50.2 GHz). The average dissipation is above −2.6 dB in the middle of the operational band.

4.3.1.3 Design and Schematic of the Q-Rx Unit Cell

Based on the V-Tx pixel design presented in the previous sections, the unit cell was modified in order to meet the specifications of the Q-Rx antenna

4.3.1.4 Simulation Result of Q-Rx Unit cell

CO-POL Dissipation level (S11 Vs Frequency) – 37.5 to 42.5 GHZ: The highest dissipation level is -2.5dB seen at 38 GHz

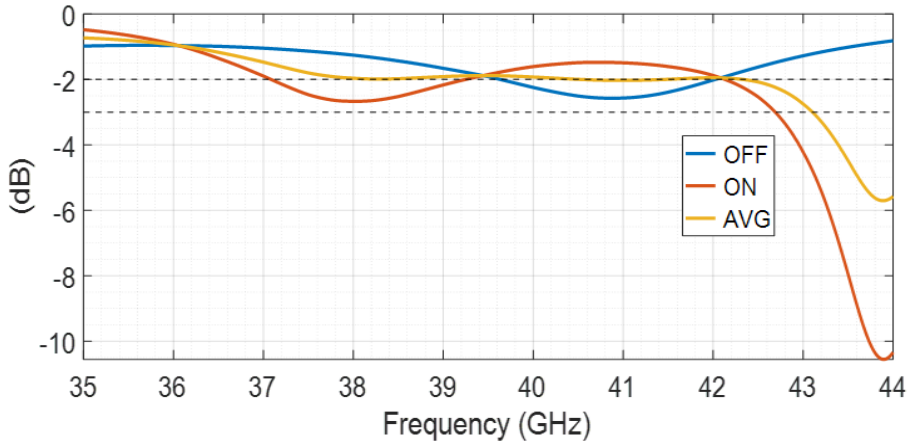

Figure 20: Simulated reflection coefficient versus frequency

CO-POL Phase difference level – 37.5 to 42.5 GHZ: The phase difference is over 140° across the band.

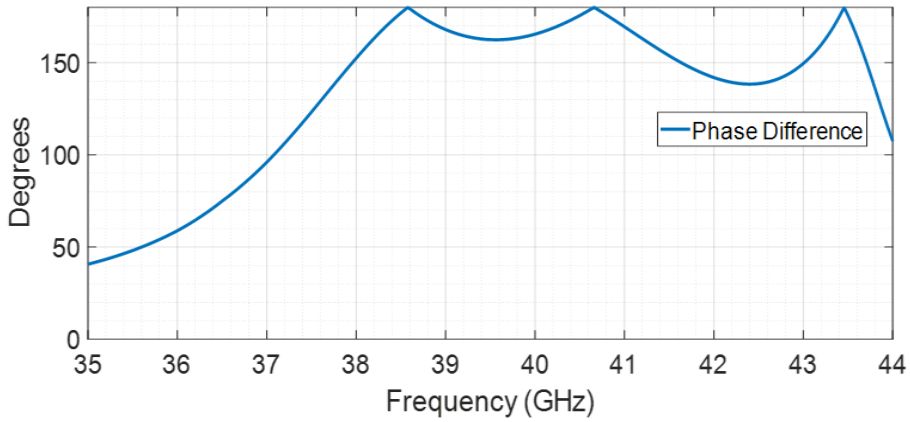

Figure 21: Simulated Phase difference versus frequency across the frequency band of Interest

Cross-POL Dissipation level (S11 Vs Frequency) – 37.5 to 42.5 GHZ : The X-pol levels for over the all the frequency band is below -20 dB. It meets the project KPI's Specification of below -15 dB

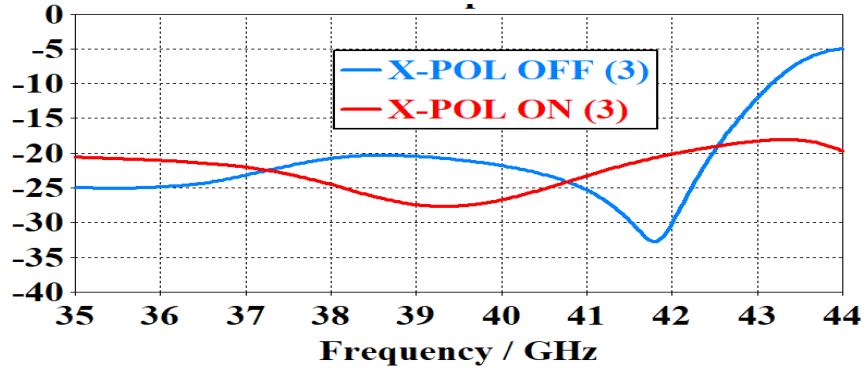

Figure 22: Simulated Cross polarization Dissipation versus Frequency

The simulation results show better than −2.5 dB and more than 140◦ phase difference in the band of interest (37.5− 42.5 GHz). The average dissipation is above −2 dB in the middle of the operational band.

METASURFACE AND MINI-METASURFACE LAYOUT DESIGN

In a standard MTS, one shift register controls 4 pixels. However, due to the small dimension of the unit cell in the Q/V band (3.4mm), placing the pixels in their standard layout orientation would result in the enable vias going directly through the shift register on the other side of the PCB. To prevent that, an alternative layout option was proposed, see figures below. In this orientation, the distance between the patches is uneven.

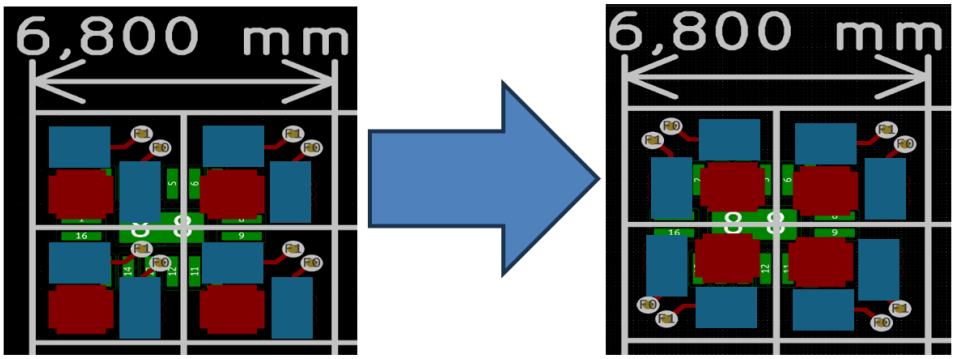

Figure 23: Layout Design of the Pixel Design

4.3.1.5 Bistatic Measurement Setup and Results

Before fabricating the complete Metasurface, we employ a Mini-Metasurface for preliminary validation. This ensures that we assess key design parameters such as dissipation level, phase difference, and resonance frequency alignment with simulation results. The Mini-Metasurface comprises a **6x6** unit cell configuration. To characterize this Mini-Metasurface, we use a Bistatic measurement setup that has essential components. This setup includes the Mini-Metasurface itself, two horn antennas for transmitting and receiving electromagnetic waves, various holders for holding different components, a dielectric lens for focusing, a Vector Network Analyzer (VNA) for precise measurements, and a power supply to control the ON/OFF states of CMOS-based switch.

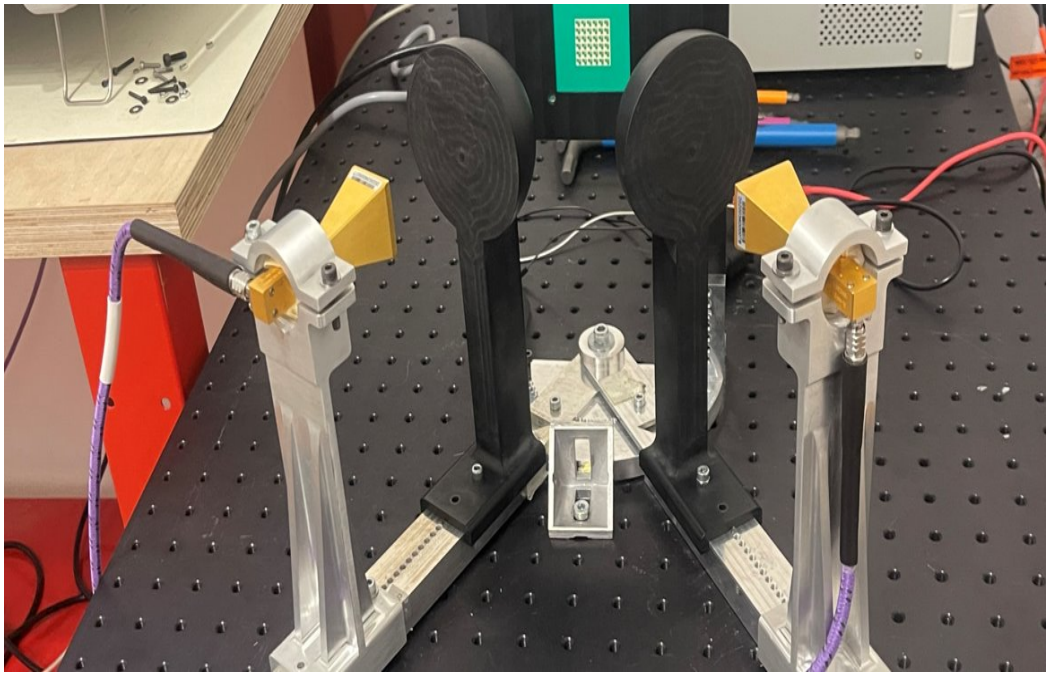

Figure 24: Bistatic Measurement Setup

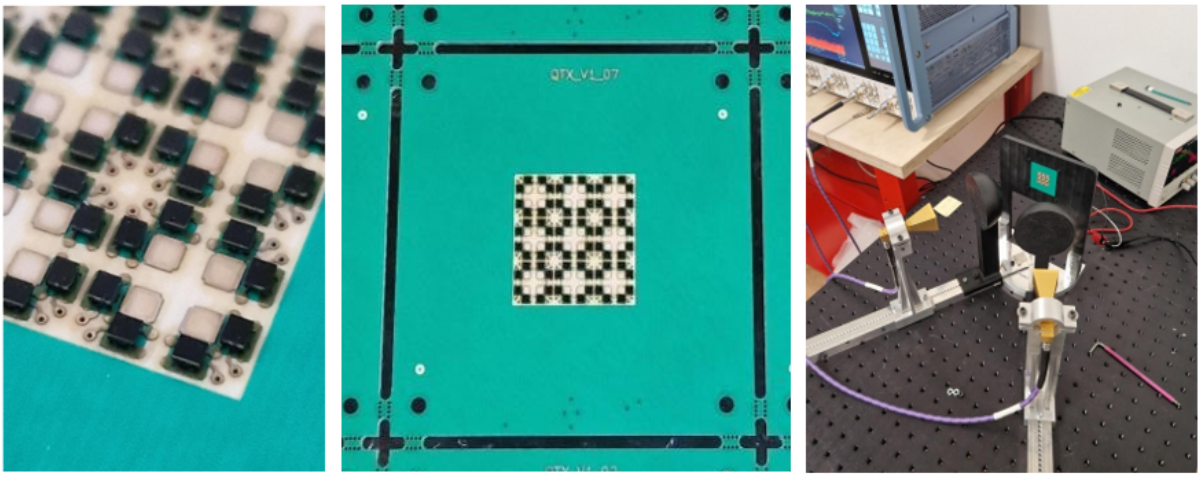

Figure 25: 6x6 mini-Metasurface

RESULTS – DISSIPATION AND PHASE DIFFERENCE:

a)

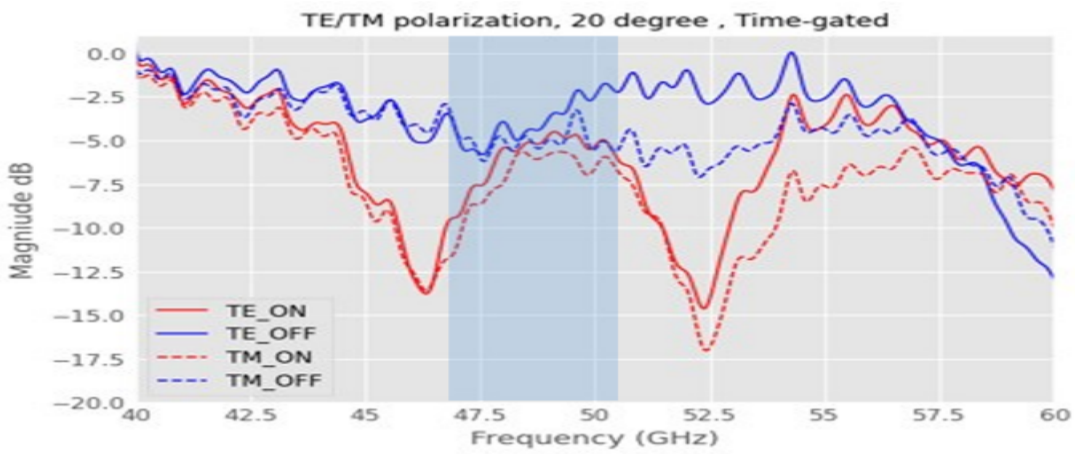

b)

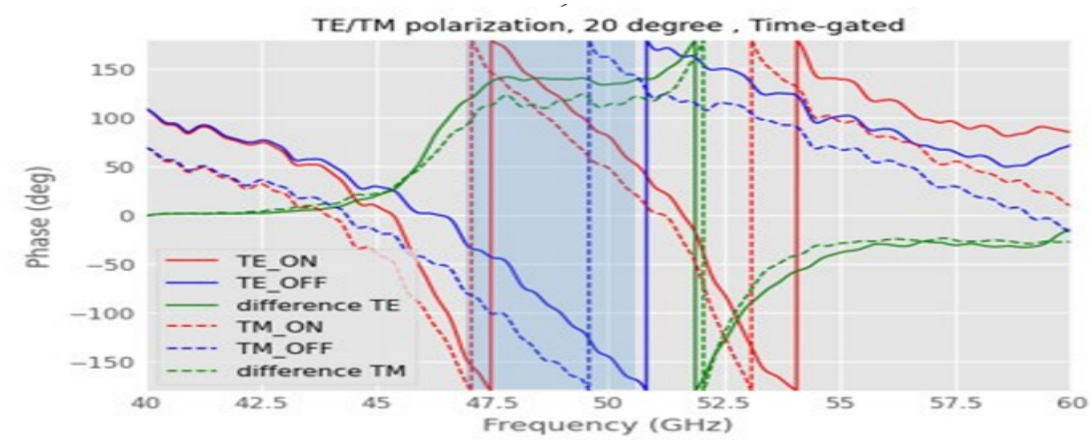

Figure 26: Measured results of the designed sample at 20◦ angle of wave incidence θ0 for the TE & TM polarization of the incident wave: (a) dissipation levels and (b) phase response

CONCLUSION

Overall, the proposed design along with the fabricated and measured samples, demonstrates an acceptable dissipation level and good phase difference between two states for two orthogonal polarizations of the incident wave. The selected Mini-Metasurface will be used for the fabrication of the full size Metasurface to be used in the leaky wave antenna technology for the proof-of-concept demonstration of the antenna operating at Q/V bands.

4.3.2 Antenna Feeder System: Simulation

The designed antenna feeder system has two subsystems:

1. H-plane splitter.
2. Radiating unit-cell (Tx and Rx).

4.3.2.1 H-Plane Splitter

It is the most critical subsystem, as it is the main building block of the entire corporate feeding network. The design is shown in Figure 16.

Three λ/4 matching sections are used. The cutoff frequency of the waveguide (WG) is 31.3336 GHz. The band of interest for this project is from 37.5 GHz to 50.2 GHz. The subsystem is simulated, and its results are reported in Figure 17. A reflection coefficient that is lower than -35 dB over the whole band of interest is noticed. This ensures a very stable operation, and results in a semi-transparent subsystem.

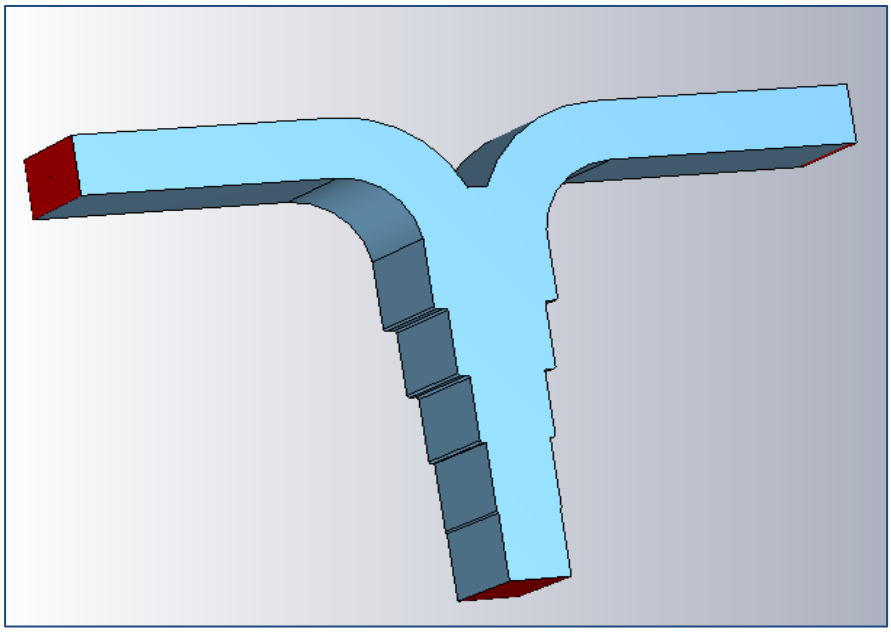

Figure 27: H-plane splitter with three λ/4 matching sections.

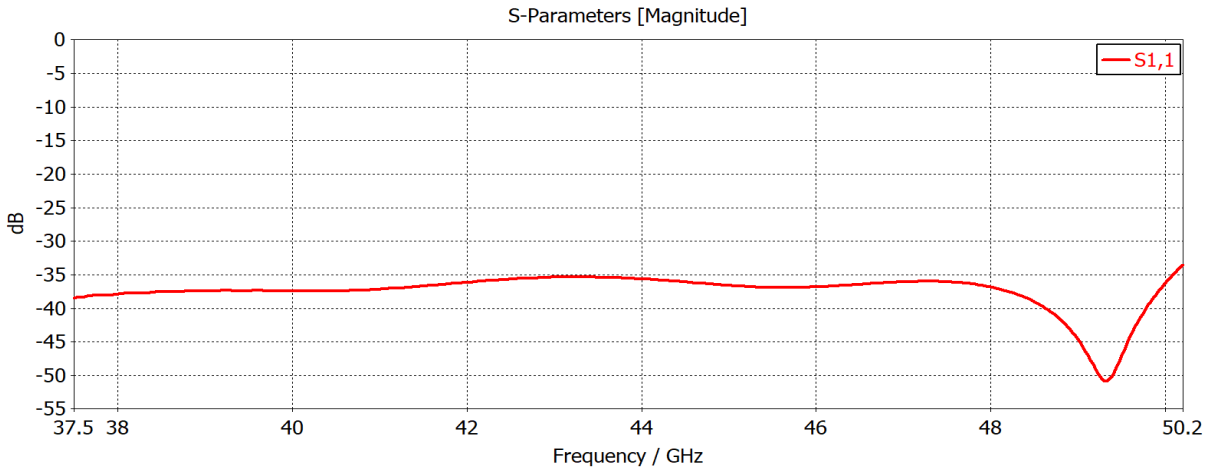

Figure 28: Simulated reflection coefficient of H-plane splitter. A reflection coefficient that is lower than -35 dB over the whole band of interest is noticed.

4.3.2.2 Radiating Unit-Cell

This section presents the radiating unit cell (subsystem) design and simulation results. Figure 29. shows images of the subsystem. Two radiating unit cells were designed, one for the RX

antenna and the other for the TX antenna. The RX subsystem is matched using four λ/4 sections, The TX subsystem is matched using three λ/4 sections, A 6 mm, why 6mm aperture is considered for both subsystems. The radiating unit cell can also be referred to as a discrete source (DS).

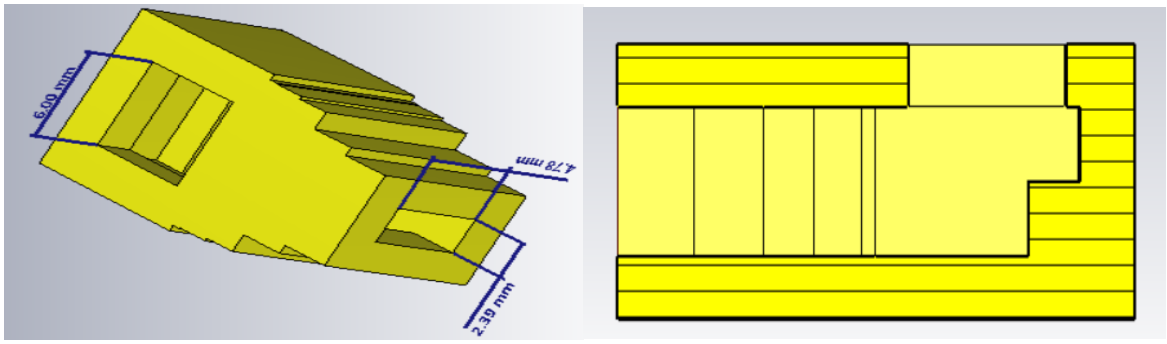

Figure 29: RX DS showing WG and aperture dimensions (a) and (b) cross-section (four λ/4 matching sections are considered).

1. RX Q BAND (37.5-42.5 GHZ)

The RX band of interest is from 37.5 GHz to 42.5 GHz. The reflection coefficient of the RX element is lower than -27.5 dB, over the band of interest as shown in Figure 19.

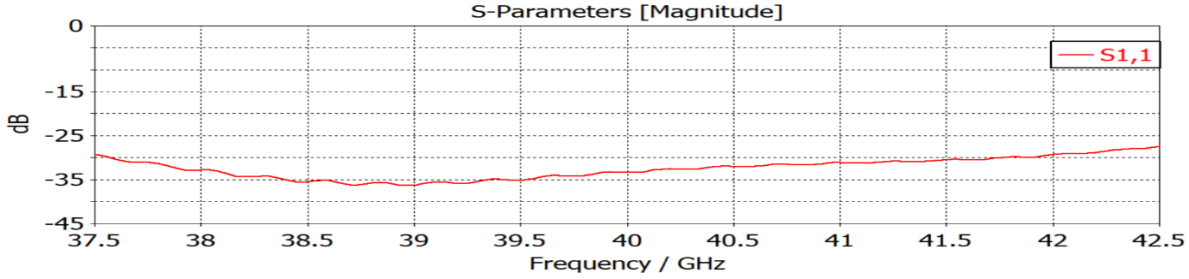

Figure 30: Simulated reflection coefficient of RX DS. A reflection coefficient of lower than -27.5 dB, over the band of interest is noticed.

2. TX V BAND (47.2-50.2 GHZ)

The TX band of interest is 47.2 GHz to 50.2 GHz. For the TX, the reflection coefficient is lower than -28.5 dB over the band of interest as shown in Figure 20.

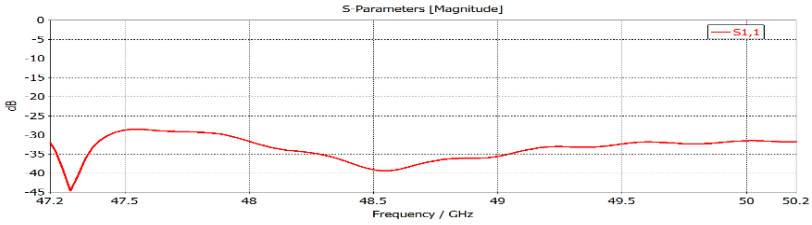

Figure 31: Simulated reflection coefficient of TX DS. A reflection coefficient of lower than -28.5 dB, over the band of interest is noticed.

4.3.2.3 KPIs

Two leakage KPI's are computed either using the magnitudes of the E-field (1) or using the square of the magnitudes of the E-field (2). The results will be presented in the following subsections.

$$Leakage\ KPI\ (\%) = \frac{|E_{Aperture}|}{|E_{Aperture}|+|E_{MTS}|} \times \quad 100\% \qquad (1)$$

$$Leakage\ KPI\ (\%) = \frac{|E_{Aperture}|^2}{|E_{Aperture}|^2+|E_{MTS}|^2} \times 100\% \qquad (2)$$

Where $|E_{Aperture}|$ is the magnitude of the E-field at the aperture level and $|E_{MTS}|$ is the magnitude of the E-field at the metasurface (MTS) level. What does it mean aperture level, and Metasurface level

To compute the leakage KPI's, we considered 2 cases where the distances from the aperture or MTS to the DS is either (*d_stp)* is either 3 mm or 3 cm.

4.3.2.4 RX KPIs

The KPIs are calculated for the following frequencies: 37.5 GHz (minimum), 40.5 GHz and 42.5 GHz (maximum). Results are reported in Table 1. (below) where d_stp is the distance from the aperture or MTS to the DS.

Table 21: RX Leakage KPIs for different frequencies and d_stp

Frequency [GHz]	***37.5***	***38.5***	***39.5***	***40.5***	***41.5***	***42.5***
Leakage KPI [%] (1) [d_stp=3 mm]	*10.1*	*9.85*	*9.52*	*9.24*	*8.9*	*8.59*
Leakage KPI [%] (2) [d_stp=3 mm]	*1.25*	*1.18*	*1.1*	*1.03*	*0.94*	*0.87*
Leakage KPI [%] (1) [d_stp=3 cm]	*12.3*	*11.8*	*11.4*	*10.94*	*10.38*	*9.96*
Leakage KPI [%] (2) [d_stp=3 cm]	*1.91*	*1.76*	*1.63*	*1.49*	*1.33*	*1.21*

4.3.2.5 TX KPIs

The KPIs are calculated for the following frequencies: 47.2 GHz (minimum), 49.2 GHz and 50.2 GHz (maximum). Results are reported in Table 21. (below) where d_stp is the distance from the aperture or MTS to the DS.

Table 22: TX Leakage KPIs for different frequencies and d_stp

Frequency [GHz]	***47.2***	***49.2***	***50.2***
Leakage KPI [%] (1) [d_stp=3 mm]	*7.53*	*6.37*	*6.10*
Leakage KPI [%] (2) [d_stp=3 mm]	*0.66*	*0.46*	*0.42*
Leakage KPI [%] (1) [d_stp=3 cm]	*7.46*	*7.13*	*7.37*
Leakage KPI [%] (2) [d_stp=3 cm]	*0.65*	*0.59*	*0.63*

4.3.2.6 Full Antenna Feeder System

The two antenna feeder systems designed and analysed are the:

1. Rx antenna feeding system (37.5-42.5 GHz)
2. Tx antenna feeding system (47.2-50.2 GHz)

4.3.2.7 Tx antenna feeding system (47.2-50.2 GHz)

Figure 32 shows the Tx Antenna Feeder System, The cavity measures (210 mm × 210 mm × 43.78 mm). The Return loss of the feeding system is shown in Figure 22. A reflection coefficient that is lower than -20 dB over the whole band of interest is noticed.

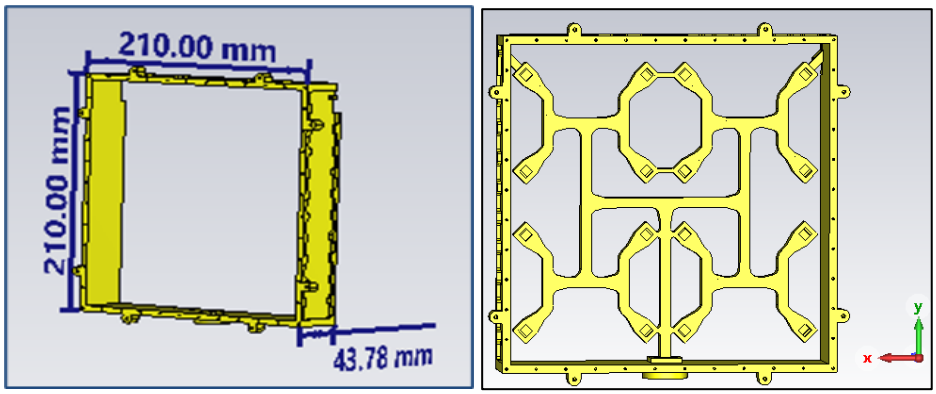

Figure 32: Tx Feeding System: (a) cavity dimensions (b) cavity with 16 DS

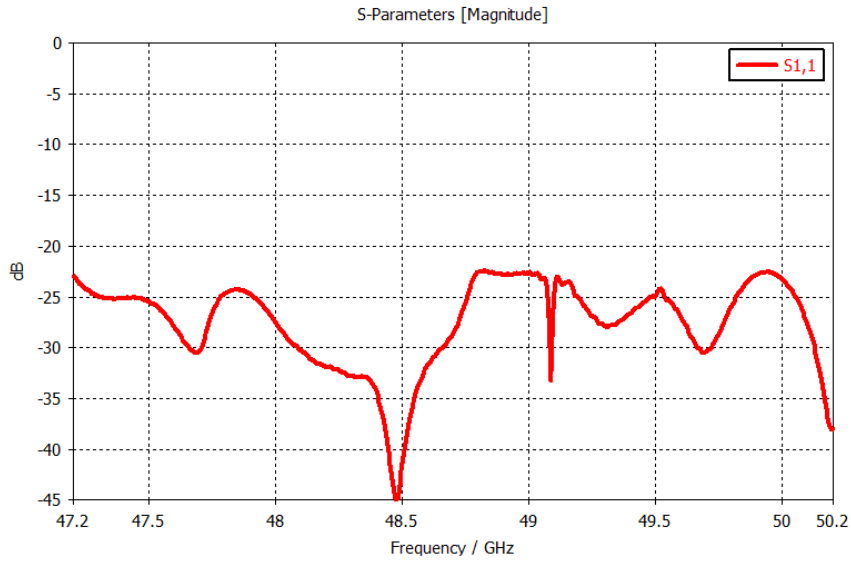

Figure 33: Simulated reflection coefficient of the Tx Feeding system. A reflection coefficient that is lower than -20 dB over the whole band of interest is noticed.

.

V-TX FEEDING SYSTEM KPIS

Two KPIs are evaluated for the AFS are the Uniformity of the field (UOF) and Leakage. UOF is defined as the ratio of the standard deviation of E-tan and its mean value measured at the MTS plane. Leakage is the ratio of the power measured at the Aperture plane and the total measured power (at both planes).

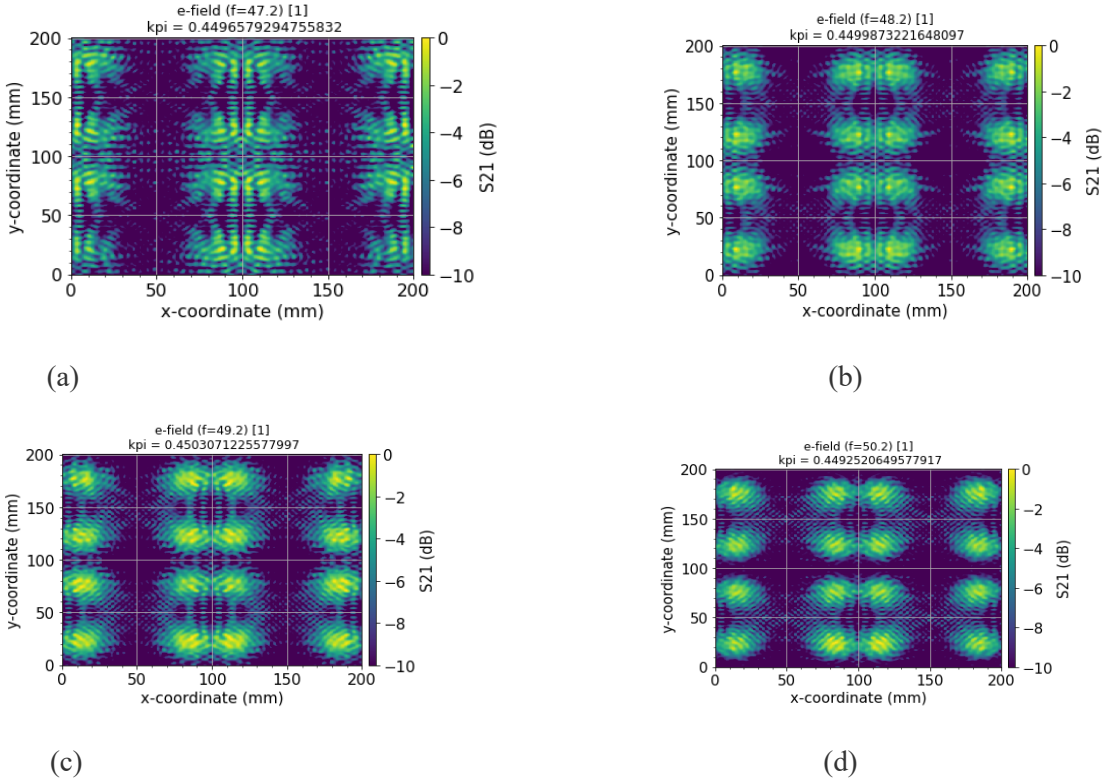

Figure 34: TX Uniformity of the Fields at (a) 47.2 GHz (b) 48.2 GHz (c) 49.2 GHz and (d) 50.2 GHz.

Table 23: TX Feeding System Leakage KPIs for different frequencies.

Frequency [GHz]	***47.2***	***48.2***	***49.2***	***50.2***
UOF	*0.45*	*0.45*	*0.45*	*0.45*
Leakage KPI [%]	*4.93*	*3.88*	*3.82*	*3.36*

4.3.2.8 Rx antenna feeding system (37.5-42.5 GHz)

Figure 35 shows the Rx AFS. The cavity measures (210 mm × 210 mm × 43.78 mm). The Return loss of the feeding system is shown in Figure 25. A reflection coefficient that is lower than -20 dB over the whole band of interest is noticed.

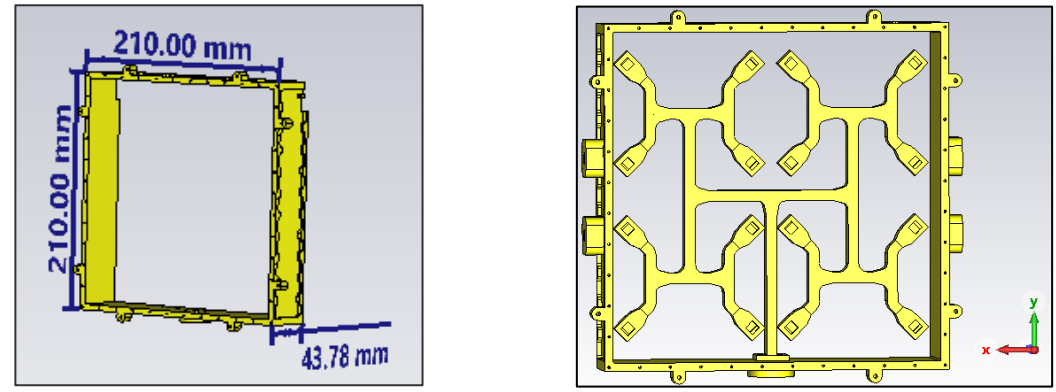

(a) (b)

Figure 35: Rx Feeding System: (a) cavity dimensions (b) cavity with 16 DS

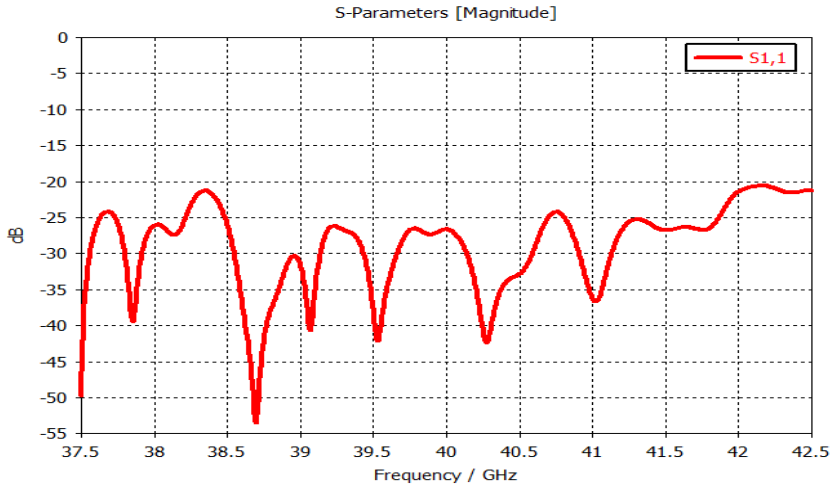

Figure 36: Simulated reflection coefficient of the Rx AFS. A reflection coefficient that is lower than -20 dB over the whole band of interest is noticed.

Q-Rx FEEDING SYSTEM KPIS

Two KPIs are evaluated for the AFS are the UOF and Leakage.

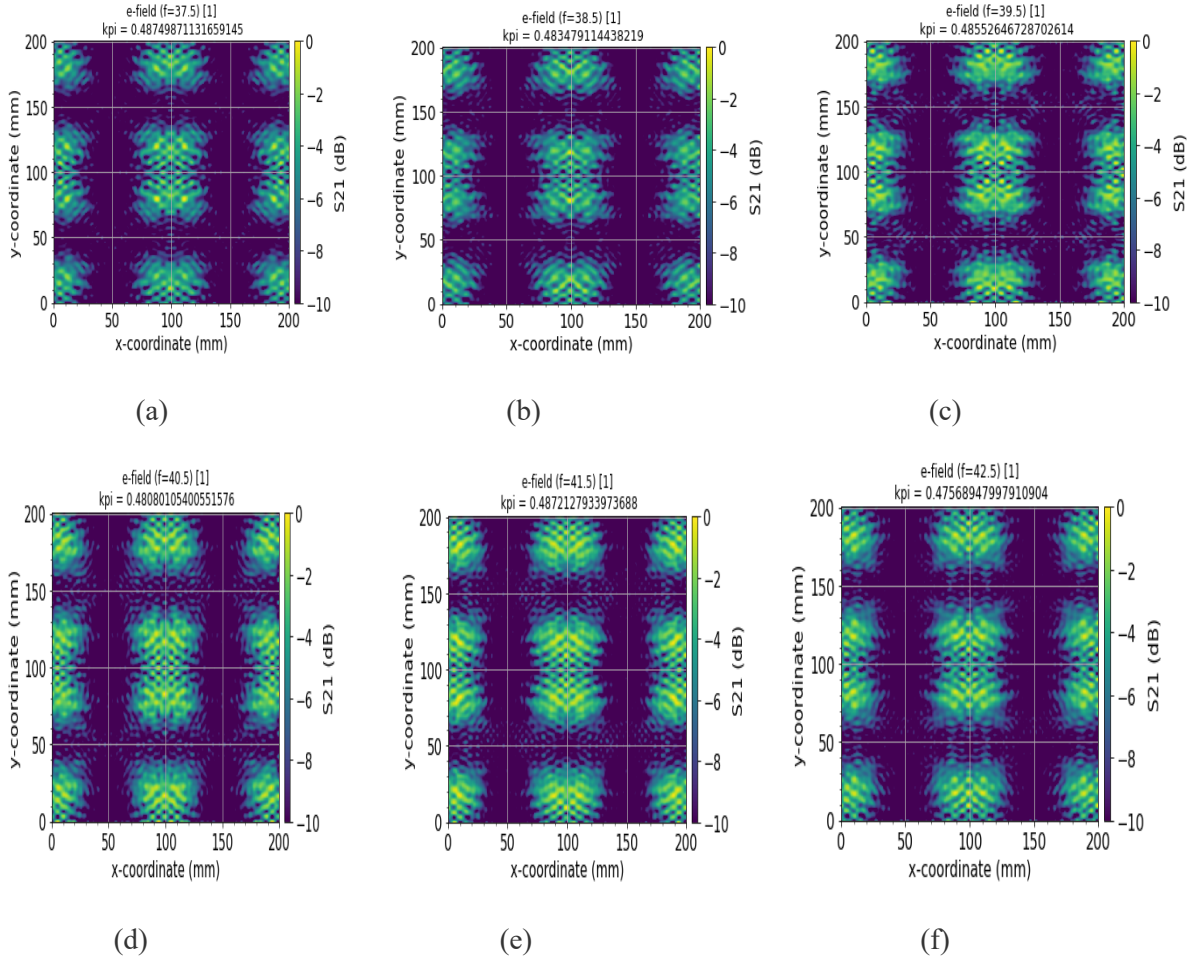

Figure 37: RX UOF at (a) 37.5 GHz (b) 38.5 GHz (c) 39.5 GHz (d) 40.5 GHz (e) 41.5 GHz and (f) 42.5 GHz

Table 24: RX Feeding System Leakage KPIs for different frequencies.

Frequency [GHz]	***37.5***	***38.5***	***39.5***	***40.5***	***41.5***	***42.5***
UOF	*0.49*	*0.48*	*0.49*	*0.48*	*0.49*	*0.48*
Leakage KPI [%]	*7.75*	*8.13*	*9.08*	*6.63*	*6.15*	*5.20*

For the Rx AFS best UOF of 0.48 was observed at (38.5 GHz, 40.5 GHz, and 42.5 GHz).

4.3.3 Antenna Feeder System: Characterization

4.3.3.1 S11 (Return Loss)

The Return Loss and the mismatching factor are shown in Figure 38(a) and in Figure 38(b), respectively.

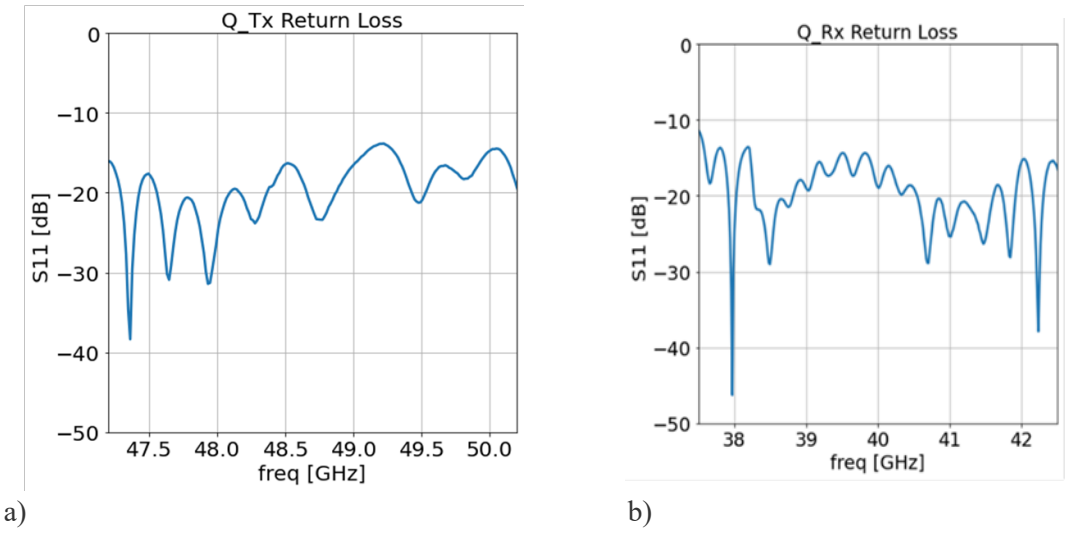

a) b)

Figure 38: Measured return loss (a) Tx (b) Rx.

The measured return loss shows a good result which is below the -15 dB for almost the whole frequency bands of interest for the Tx and Rx AFSs.

4.3.3.2 Near-Field Planar Scan Results

The planar near-field (NF) scans are performed at the desired planes.

The Tx near-field scan plots are presented in the tables provided below, along with the far-field plots (near-field to far-field transformation) at 47.2 GHz (3.1.2.1) and 49.2 GHz (3.1.2.2) covering the whole desired V band.

The Rx near-field scan plots are presented in the tables provided below, along with the far-field plots (near-field to far-field transformation) at 37.5 GHz (3.1.2.1) and 40.5 GHz (3.1.2.1) covering the whole desired V band.

4.3.3.3 FREQUENCY 47.2 GHZ

1. NORMALIZATION WITH -10 DB

The NF measured results which are normalized with -10 dB are shown in Figure 39.

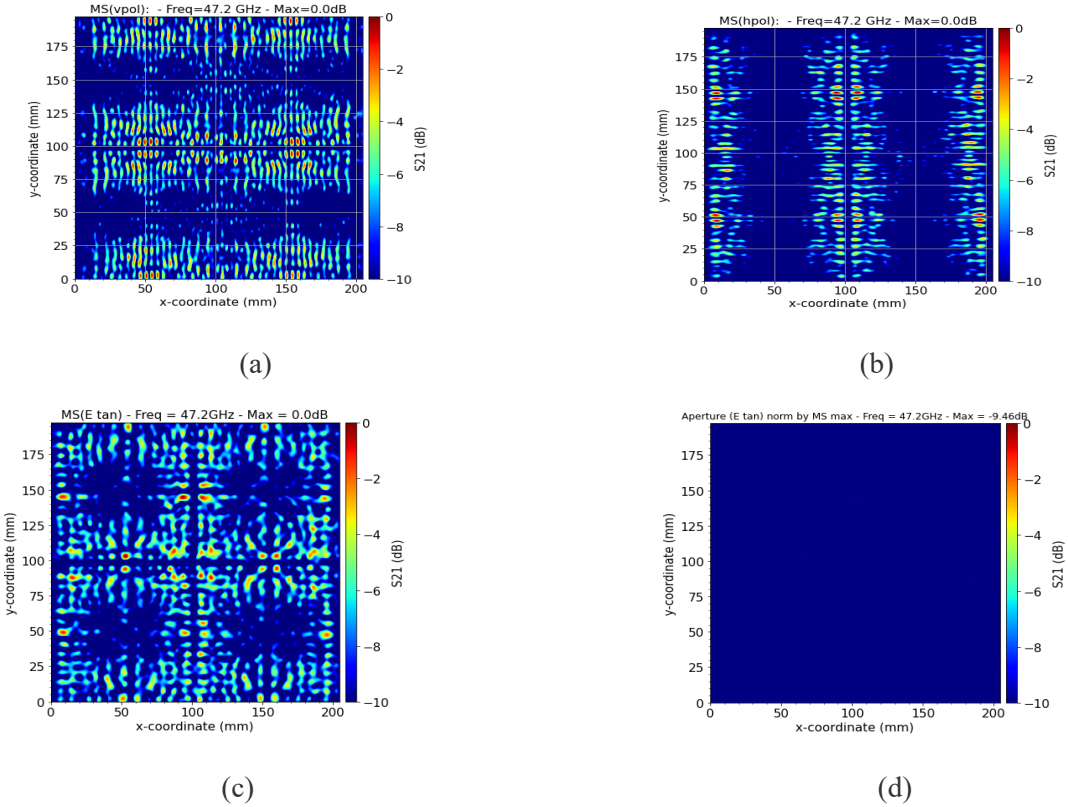

Figure 39: NF scan results at 47.2 GHz normalized with -10 dB: (a) V-pol, (b) H-pol and (c) Total tangential E-fields at the MTS plane. (d) Total tangential E-fields at the mask plane.

2. NORMALIZATION WITH -20 DB

The NF measured results which are normalized with -20 dB are shown in figure 40 below.

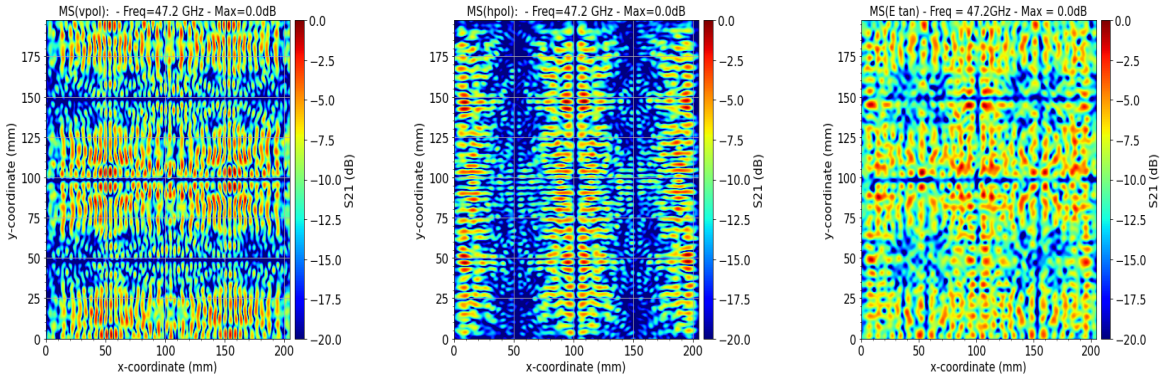

Figure 40: NF scan results at 47.2 GHz normalized with -20 dB: (a) V-pol, (b) H-pol and c) Total tangential E-fields at the MTS plane.

4.3.3.4 FREQUENCY 49.2 GHZ

1. NORMALIZATION WITH -10 DB

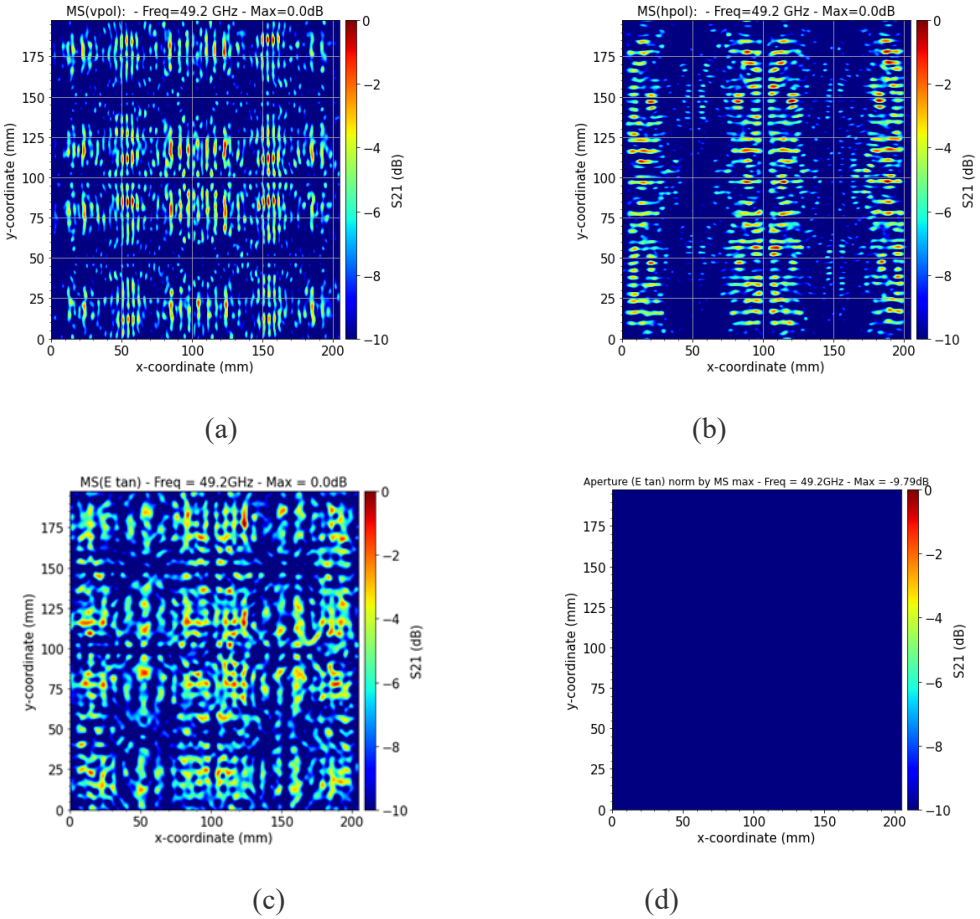

Figure 41: NF scan results at 49.2 GHz normalized with -10 dB: (a) V-pol, (b) H-pol and (c) Total tangential E-fields at the MTS plane. (d) Total tangential E-fields at the mask plane.

2. NORMALIZATION WITH -20 DB

The NF measured results which are normalized with -20 dB are shown in Figure 31.

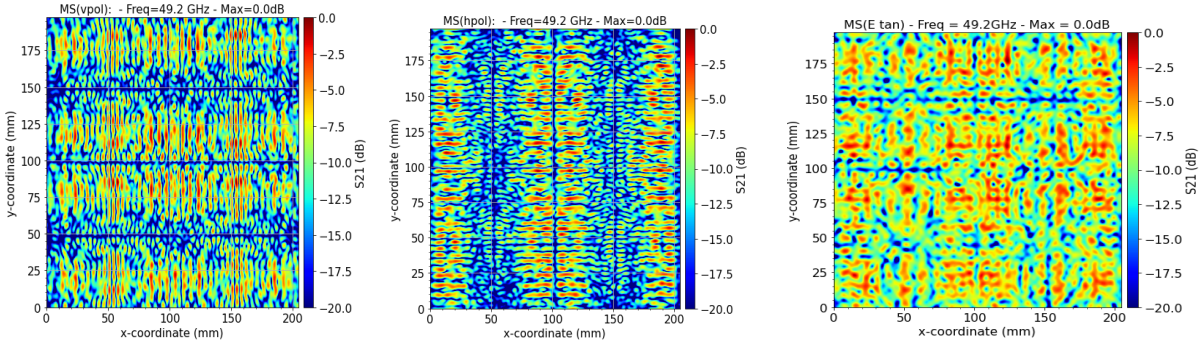

Figure 42: NF scan results at 49.2 GHz normalized with -20 dB. (a) V-pol, (b) H-pol and (c) Total tangential E-fields at the MTS plane.

4.3.3.5 Frequency 37.5 GHz

1. NORMALIZATION WITH -10 DB

The NF measured results which are normalized with -10 dB are shown in Figure 43 below.

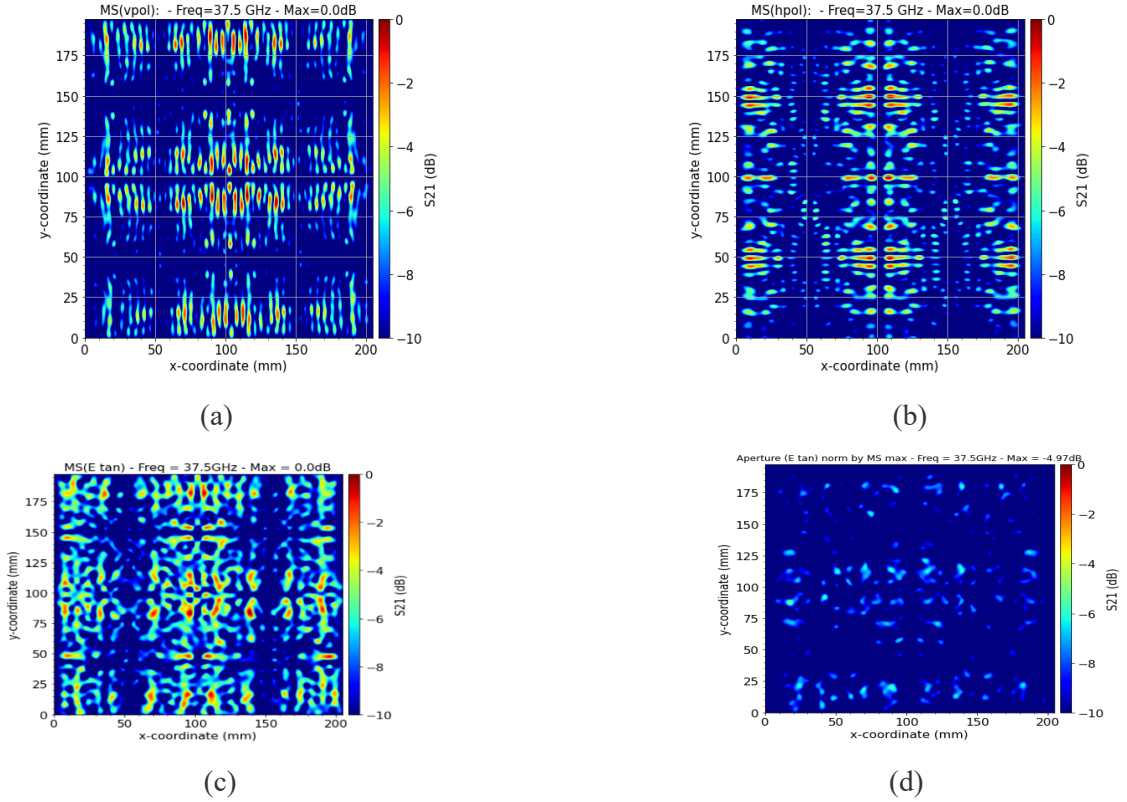

Figure 43: NF scan results at 37.5 GHz normalized with -10 dB: (a) V-pol, (b) H-pol and (c) Total tangential E-fields at the MTS plane. (d) Total tangential E-fields at the mask plane.

2. NORMALIZATION WITH -20 DB

The NF measured results which are normalized with -20 dB are shown in 44 below.

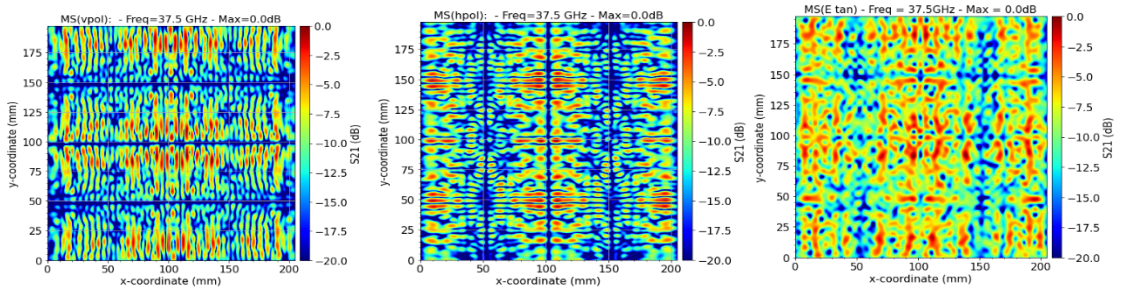

Figure 44: NF scan results at 37.5 GHz normalized with -20 dB: (a) V-pol, (b) H-pol and (c) Total tangential E-fields at the MTS plane.

The normalized field at the aperture level is not shown here since it has no interest.

4.3.3.6 Frequency 40.5 GHz

1. NORMALIZATION WITH -10 DB

The NF measured results which are normalized with -10 dB are shown in Figure 34 below.

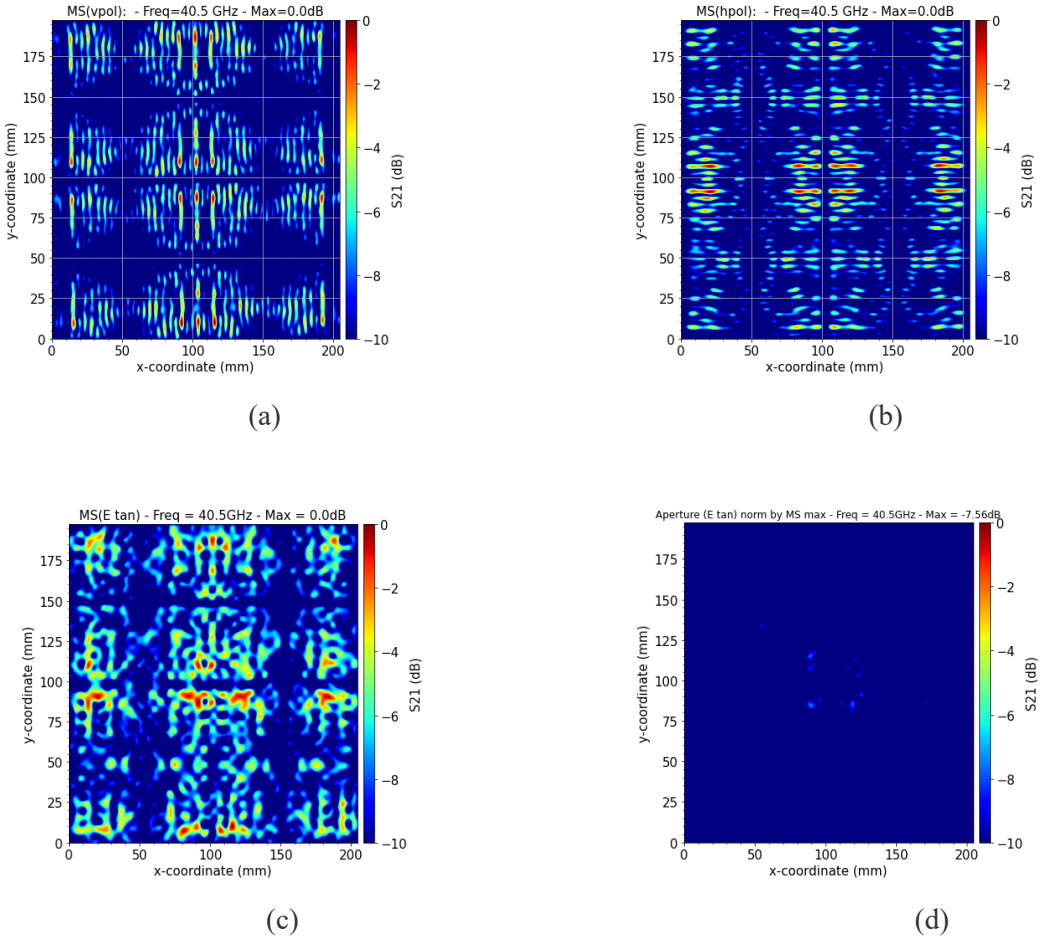

Figure 45: NF scan results at 40.5 GHz normalized with -10 dB: (a) V-pol, (b) H-pol and (c) Total tangential E-fields at the MTS plane. (d) Total tangential E-fields at the mask plane.

2. NORMALIZATION WITH -20 DB

The NF measured results which are normalized with -20 dB are shown in Figure 35 below.

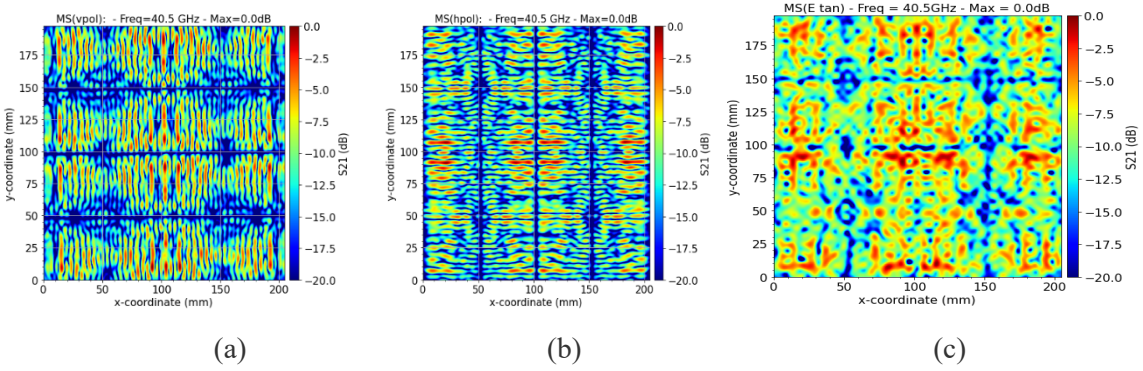

Figure 46 NF scan results at 40.5 GHz normalized with -20 dB: (a) V-pol, (b) H-pol and (c) Total tangential E-fields at the MTS plane.

The normalized field at the aperture level is not shown here since it has no interest.

4.3.3.7 KPIs and Direct leakage

The UOF is defined by the ratio of the standard deviation of E-tan and its mean value measured at the MTS plane.

Table 25: Summary of Tx AFS KPI: UOF and spillover at predefined frequency points

	47.2 GHz	48.2 GHz	49.2 GHz	50.2 GHz
UOF	0.41	0.39	0.39	0.39
Spillover (%)	8.0	8.13	9.1	8.73

Table 26: Summary of Rx AFS KPI: UOF and spillover at predefined frequency points.

	37.5 GHz	38.5 GHz	39.5 GHz	40.5 GHz	41.5 GHz	42.5 GHz
UOF	0.41	0.42	0.41	0.41	0.40	0.40
Spillover (%)	9.16	8.9	9.18	6.4	7.36	8.57

4.3.3.8 Conclusion

1. The measured return loss is below -15 dB for almost the entire QV band.
2. Tm
3. The best Rx KPI (0.40) was found at 41.5 GHz and 42.5 GHz with a direct leakage of around 7.36 % and 8.57% respectively. Meanwhile, the lowest direct leakage (6.4 %) can be found at 40.5 GHz with a KPI of about 0.41.

4.3.4 Antenna Mask

This part of the antenna allows us to fix a desired transmitted level of power and reflect the remaining part towards the Metasurface. Multiple reflections accrue then between the Metasurface and the mask.

4.3.4.1 QRx and VTx masks design

The technical details of the two masks are:

1. Frequency of interest: Q-Rx => [37.5 GHz – 42.5 GHz]
   Q-Tx => [47.2 GHz – 50.2 GHz]
2. Geometry: Flat, uniform and one layer PCB based.
3. Dissipation: 0.01
4. Transmission: 65%
5. CrossPol < -20 dB
6. Material: Rogers 4003C

Some KPIs need to be reached in order to validate the designed masks. The fabrication of the mask is based on a fixed goal (% of transmission) and KPIs reflecting the TE and TM modes symmetry as function of incidence angle Theta.

4.3.5 Antenna Mask Characterization

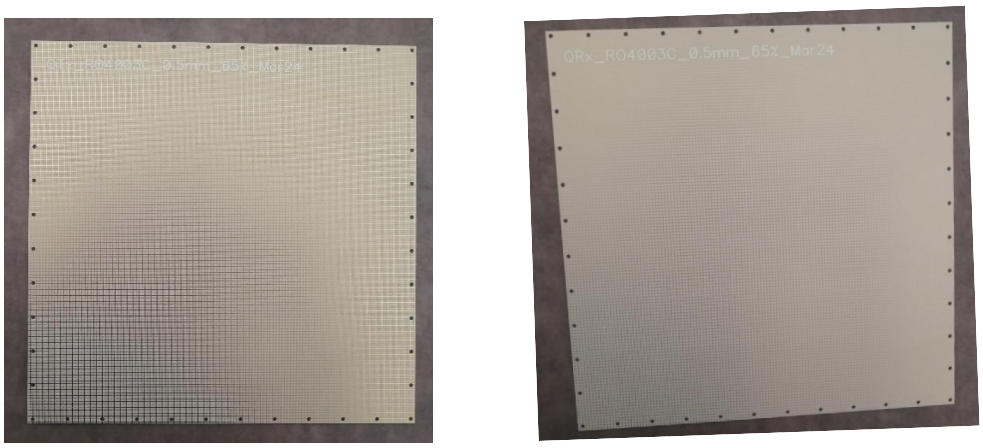

Figure 47: VTx (left) and QRx (right) masks

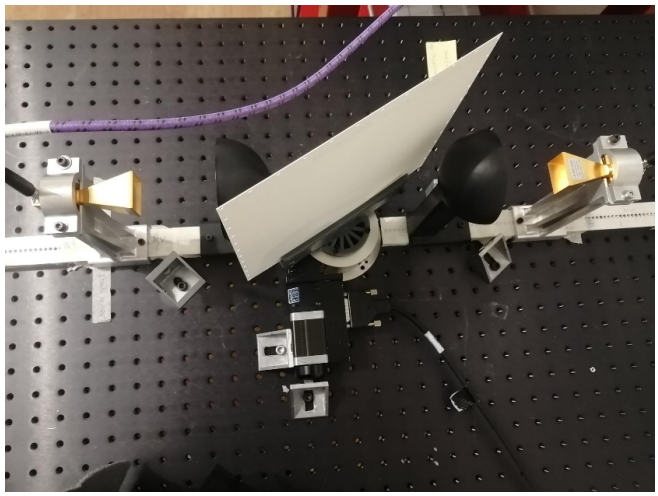

Figure 48: Masks characterization setup

Both masks transmission coefficients were measured for different angles [0°-50°]. Results are presented in table below and compared to simulation.

Table 27: QRx and VTx characterization results compared to simulation

	Mask QRx [BW : 12%]	**Mask VTx [BW : 6%]**
Measurement	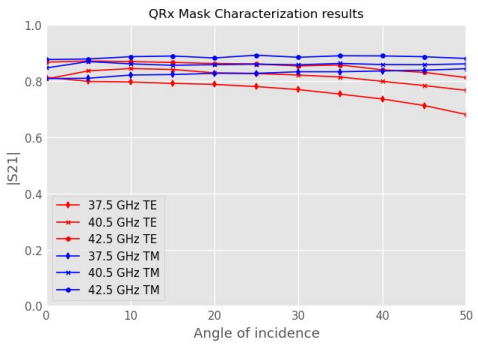	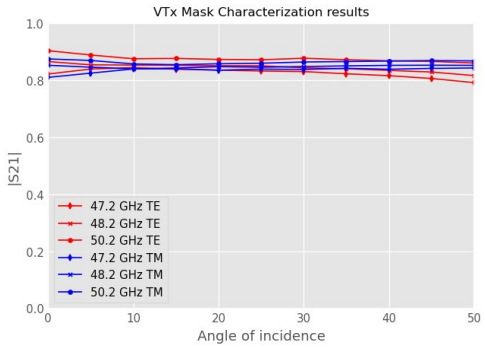
Simulation	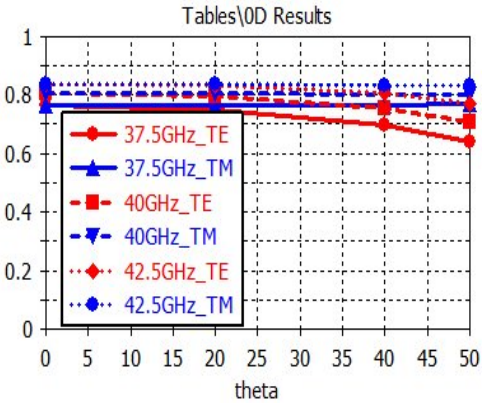	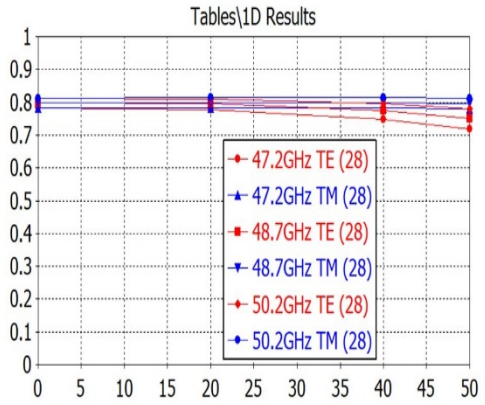

The desired transmission level of power was 0.65% (0.8% S21 level).

Both masks present good coherence between measurement and simulation result with a larger dispersion in measurement estimated around 5% for both masks.

4.4 CONCLUSION

A novel Q/V-band 1-bit reconfigurable metasurface for 6G-NTN applications has been designed, simulated and measured. Overall, the proposed design along with the fabricated and measured samples, demonstrates an acceptable dissipation level and good phase difference between two states for two orthogonal polarisations of the incident wave. The selected mini-metasurface will be used for the fabrication of the full size metasurface to be

used in the leaky wave antenna technology for the proof-of-concept demonstration of the antenna operating at Q/V bands.

Both Q/V masks present good coherence between measurement and simulation result with a larger dispersion in measurement estimated around 5% for both masks.

Antenna Feeder System for both Q and V band has been designed, simulated and measured. Overall, the proposed design along with the fabricated and Measured sample meet the Specification of the project and already for the Full antenna systems.

4.5 FUTURE WORK

1. The full antenna characterization will be performed.
2. The second iteration of the Metasurface design using PIN diodes will be completed.

5 SERVICE CAPABILITY OF UE TYPES

For the final report feedback from the EAB will be incorporated related to the service capabilities of UE types depending on antennas and their applicability for the various use cases. Furthermore, the identified challenging areas and operation modes will be assessed and discussed.

Note: The overall considerations may also be included in the general 6G-NTN system evaluation part, as more aspects than only the terminal need to be considered here.

6 OUTLOOK TO FINAL VERSION OF THE REPORT

The current version of the report reflects the intermediate state concerning terminal analysis. especially focusing on innovative antenna design and the investigations thereof. In alignment with use case and project requirement analysis (WP2.1, WP2.2 and WP2.3) side conditions for said analysis were considered and first simulations and measurements. These promising results were compared against today's state-of-the art antenna performance considered by 3GPP for NTN. A clear performance improvement leading to higher throughput in the analyzed area could be observed.

Further studies will be conducted for smaller geometry, as also indicated by the use case analysis in WP2.2, to be able to address more use cases being important for economic scale of 6G-NTN besides fully integrated designs. In addition, C-band analysis, which was concluded on first analysis to be second priority, will be performed if time allows. Furthermore, general aspects related to terminal sustainability (e.g., energy efficiency and recyclability) will be addressed in more details for the final delivery.

7 INTERMEDIATE SUMMARY

The future work in this project part will proceed with identified major antenna investigation for terminals as innovative field offering most improvement potential for 6G NTN. First promising design and measurements were made, further tasks will study different maximum sizes for the so far addressed Q/V band, but also perform adaptations to the design to make it suitable for further bands to be able to address a larger amount of use cases.

Based on the achieved terminal results calculations and studies will be made to evaluate the 6G NTN system throughput and capacity. These considerations and evaluations will not only be made for the new and innovative antenna designs, but also for the group of NTN terminals which have a fully integrated common front-end design for handhelds (NTN/TN dual use). The common design for handhelds was identified to be a major driver for distribution and hence also critical for the 6G NTN system even though not preparing any innovation potential on the terminal side but 6G NTN performance improvements will be delivered from other 6G NTN system components.

The so far observed performance increase in Q/V band antenna simulation results and measurements indicates that with geometrical dimension and weight being acceptable for many use cases (20x20cm) and use case scenarios, a significant performance increase especially for 6G wideband NTN services can be achieved. Further investigation will focus on smaller geometries and additional bands to further enhance the market potential for 6G overall systems by innovative antenna design for terminals.

8 REFERENCES

[1] OpenAMIP Standard, online available at https://www.idirect.net/products/openamip/

[2] https://www.microwavejournal.com/articles/36358-thinkom-unveils-new-q-v-band-phased-array-satellite-antennas-for-next-generation-satellite-constellations, retrieved on June 2024

[3] Variable inclination continuous transverse stub array, US patent number US6919854B2

[4] F. Ahmed, K. Singh and K. P. Esselle, "State-of-the-Art Passive Beam-Steering Antenna Technologies: Challenges and Capabilities," in *IEEE Access*, vol. 11, pp. 69101-69116, 2023, doi: 10.1109/ACCESS.2023.3278570.

[5] Yuanzhi He, Fan Yang, Guodong Han, Yuanyuan Li, High-throughput SatCom-on-the-move antennas: technical overview and state-of-the-art, Digital Communications and Networks, 2023, ISSN 2352-8648, https://doi.org/10.1016/j.dcan.2023.11.005.

[6] G. Amendola *et al.*, "Low-Earth Orbit User Segment in the Ku and Ka-Band: An Overview of Antennas and RF Front-End Technologies," in *IEEE Microwave Magazine*, vol. 24, no. 2, pp. 32-48, Feb. 2023, doi: 10.1109/MMM.2022.3217961.

[7] T. Chaloun *et al.*, "Electronically Steerable Antennas for Future Heterogeneous Communication Networks: Review and Perspectives," in *IEEE Journal of Microwaves*, vol. 2, no. 4, pp. 545-581, Oct. 2022, doi: 10.1109/JMW.2022.3202626.

[8] W. Hong et al., "Multibeam Antenna Technologies for 5G Wireless Communications," in IEEE Transactions on Antennas and Propagation, vol. 65, no. 12, pp. 6231-6249, Dec. 2017.

[9] https://www.intelliantech.com/en/products/#

[10] https://gilat.com/technologies/defense/terminals-antennas/

[11] https://www.hanwha-phasor.com/

[12] https://www.satixfy.com/product_category/antennas/

[13] S. V. Hum and J. Perruisseau-Carrier, "Reconfigurable Reflectarrays and Array Lenses for Dynamic Antenna Beam Control: A Review

[14] Liu Shuang , Li Yin , Wong Sai-Wai , Zhang Xiao , Wang Shiyan , Fang Liang , Gao Qiang , A circularly polarized folded reflectarray antenna using a polarization-sensitive linear-to-circular polarization converter, Frontiers in Physics ,VOLUME10, YEAR 2022, DOI:10.3389/fphy.2022.983951

[15] A. Oliner and A. Hessel, “Guided waves on sinusoidally-modulated reactance surfaces,” IRE Trans. Antennas Propag., vol. TAP-7, no. 5, pp. 201–208, Dec. 1959.

[16] https://www.kymetacorp.com/solutions/?utm_medium=adwords&utm_campaign=brand&gad_source=1&gclid=CjwKCAjwmrqzBhAoEiwAXVpgonw47E94QzL_cIBGYfK_nhYr0iVyxKPHThZp78HcMQktey46AsEguxoCgEsQAvD_BwE

[17] P. Commware, “Holographic beam forming technology – Pivotal commware,” Accessed: Mar. 22, 2022.

[18] J. Ruiz-García, C. Bilitos, E. Martini, G. Toso, S. Maci and D. González-Ovejero, "Metal-only Multi-beam Fabry-Perot Antenna," *2022 16th European Conference on Antennas and Propagation (EuCAP)*, Madrid, Spain, 2022, pp. 1-4, doi: 10.23919/EuCAP53622.2022.9769193.

[19] Saeid Karamzadeh, Vahid Rafiei, and Mesut Kartal, "Beam Steering Fabry Perot Array Antenna for mm -Wave Application," *Progress In Electromagnetics Research M*, Vol. 91, 81-89, 2020. doi:10.2528/PIERM20020101

[20] https://www.all.space/products-services

[21] https://www.alcansystems.com/

[22] “The Isotropic Antenna: The Perfect Solution for Aero?”, Satellite Mobility, May 2020, retrieved on June 2024 from https://www.all.space/insights/the-isotropic-antenna-the-perfect-solution-for-aero
[23] Jakoby, R.; Gaebler, A.; Weickhmann, C. Microwave Liquid Crystal Enabling Technology for Electronically Steerable Antennas in SATCOM and 5G Millimeter-Wave Systems. *Crystals* **2020**, *10*(6), 514
[24] Amirhossein Askarian and Ke Wu, “Aperture-Shared Radiation Surface: A Promising Technique for Multifunctional Antenna Array Development,” Electromagnetic Science, vol. 1, no. 3, article no. 0030082, 2023. doi: 10.23919/emsci.2023.0008
[25] X. Artiga, "Effects of Unit Cell Enlargement and 1-Bit Quantization in 5G Linear Metasurface Antennas," *2018 European Conference on Networks and Communications (EuCNC)*, Ljubljana, Slovenia, 2018, pp. 1-9, doi: 10.1109/EuCNC.2018.8442638.
[26] Kin-Lu Wong, “Compact and Broadband Microstrip Antennas”, John Wiley & Sons, 2002, ISBNs: 0-471-41717-3 (Hardback); 0-471-22111-2 (Electronic)
[27] J. F. Zhang, Y. J. Cheng, Y. R. Ding, et al., “A dual-band sharedaperture antenna with large frequency ratio, high aperture reuse efficiency, and high channel isolation,” IEEE Transactions on Antennas and Propagation, vol. 67, no. 2, pp. 853–860, 2019.
[28] J. Zhu, Y. Yang, S. Liao, S. Li and Q. Xue, "Dual-Band Aperture-Shared Fabry–Perot Cavity-Integrated Patch Antenna for Millimeter-Wave/Sub-6 GHz Communication Applications," in *IEEE Antennas and Wireless Propagation Letters*, vol. 21, no. 5, pp. 868-872, May 2022, doi: 10.1109/LAWP.2022.3148408.
[29] M. B. Young, K. A. O'Connor and R. D. Curry, "Reducing the size of helical antennas by means of dielectric loading," *2011 IEEE Pulsed Power Conference*, Chicago, IL, USA, 2011, pp. 575-579, doi: 10.1109/PPC.2011.6191490.
[30] Tang, Xihui, Feng, Botao, Long, Yunliang, The Analysis of a Wideband Strip-Helical Antenna with 1.1 Turns, *International Journal of Antennas and Propagation*, 2016, 5950472, 7 pages, 2016. https://doi.org/10.1155/2016/5950472
[31] I. Lim and S. Lim, "Monopole-Like and Boresight Pattern Reconfigurable Antenna," in *IEEE Transactions on Antennas and Propagation*, vol. 61, no. 12, pp. 5854-5859, Dec. 2013, doi: 10.1109/TAP.2013.2283926.
[32] 3GPP TS 38.101-5 V18.5.0, "User Equipment (UE) radio transmission and reception; Part 5: Satellite access Radio Frequency (RF) and performance requirements (Release 18)"
[33] 3GPP TS 38.300 V18.1.0, "Technical Specification Group Radio Access Network; NR and NG-RAN Overall Description; Stage 2 (Release 18)"
[34] 3GPP TS 38.101-2 V18.5.0, "User Equipment (UE) radio transmission and reception; Part 2: Range 2 Standalone (Release 18)"
[35] ITU-R Recommendation SM.1541-6, "Unwanted emissions in the out-of-band domain"
[36] ITU-R Recommendation SM.329-12, "Unwanted emissions in the spurious domain"
[37] 3GPP TS 38.101-1 v18.5.0, "User Equipment (UE) radio transmission and reception; Part 1: Range 1 Standalone (Release 18)"
[38] 3GPP TS 38.101-3 v18.5.0, "User Equipment (UE) radio transmission and reception; Part 3: Range 1 and Range 2 Interworking operation with other radios (Release 18)"
[39] 3GPP TS 38.101-4 v18.5.0, "User Equipment (UE) radio transmission and reception; Part 4: Performance requirements (Release 18)"
[40] ETSI EN 302 217-4 - V2.1.1 (2017-05), "Characteristics and requirements for point-to-point equipment and antennas; Part 4: Antennas"
[41] 6G-NTN deliverable D4.4 - "Spectrum Regulation Analysis for 6G NTN Scenarios"
[42] C.-X. Wang, X. You, X. Gao, et al., “On the road to 6g: Visions, requirements, key technologies, and testbeds,” IEEE Communications Surveys Tutorials, vol. 25, no. 2, pp. 905–974, 2023. DOI: 10.1109/ COMST.2023.3249835.

[43] A. Guidotti, A. Vanelli-Coralli, V. Schena, et al., “The path to 5g-advanced and 6g non-terrestrial network systems,” in 2022 11th Advanced Satellite Multimedia Systems Conference and the 17th Signal Processing for Space Communications Workshop (ASMS/SPSC), 2022, pp. 1–8. DOI: 10.1109/ASMS/SPSC55670.2022.9914764.
[44] About 6g-ntn, 6G-NTN, [Online]. Available: https://www.6g- ntn.eu/ about-6g-ntn/, Accessed: March 15, 2024.
[45] Q. Wu, S. Zhang, B. Zheng, C. You, and R. Zhang, “Intelligent reflecting surface aided wireless communications: A tutorial,” Jul. 2020.
[46] M. A. ElMossallamy, H. Zhang, L. Song, K. G. Seddik, Z. Han, and G. Y. Li, “Reconfigurable intelligent surfaces for wireless communications: Principles, challenges, and opportunities,” IEEE Transactions on Cognitive Communications and Networking, vol. 6, no. 3, pp. 990–1002, 2020. DOI: 10.1109/TCCN.2020.2992604.
[47] C. Pan, H. Ren, K. Wang, et al., “Reconfigurable intelligent surfaces for 6g systems: Principles, applications, and research directions,” IEEE Communications Magazine, vol. 59, no. 6, pp. 14–20, 2021. DOI: 10. 1109/MCOM.001.2001076.
[48] M. Jian, G. C. Alexandropoulos, E. Basar, et al., “Reconfigurable intelligent surfaces for wireless communications: Overview of hardware designs, channel models, and estimation techniques,” Intelligent and Converged Networks, vol. 3, no. 1, pp. 1–32, 2022. DOI: 10 . 23919 / ICN.2022.0005.
[49] J.-B. Gros, V. Popov, M. A. Odit, V. Lenets, and G. Lerosey, “A reconfigurable intelligent surface at mmwave based on a binary phase tunable metasurface,” IEEE Open Journal of the Communications Society, vol. 2, pp. 1055–1064, 2021. DOI: 10.1109/OJCOMS.2021. 3076271.
[50] J.-B. Gros, V. Popov, M. Odit, R. Faggiani, and G. Lerosey, “Electronically reconfigurable leaky cavity antennas,” 2021

